Volume 7, 2022

CRMD

GeoPatterns

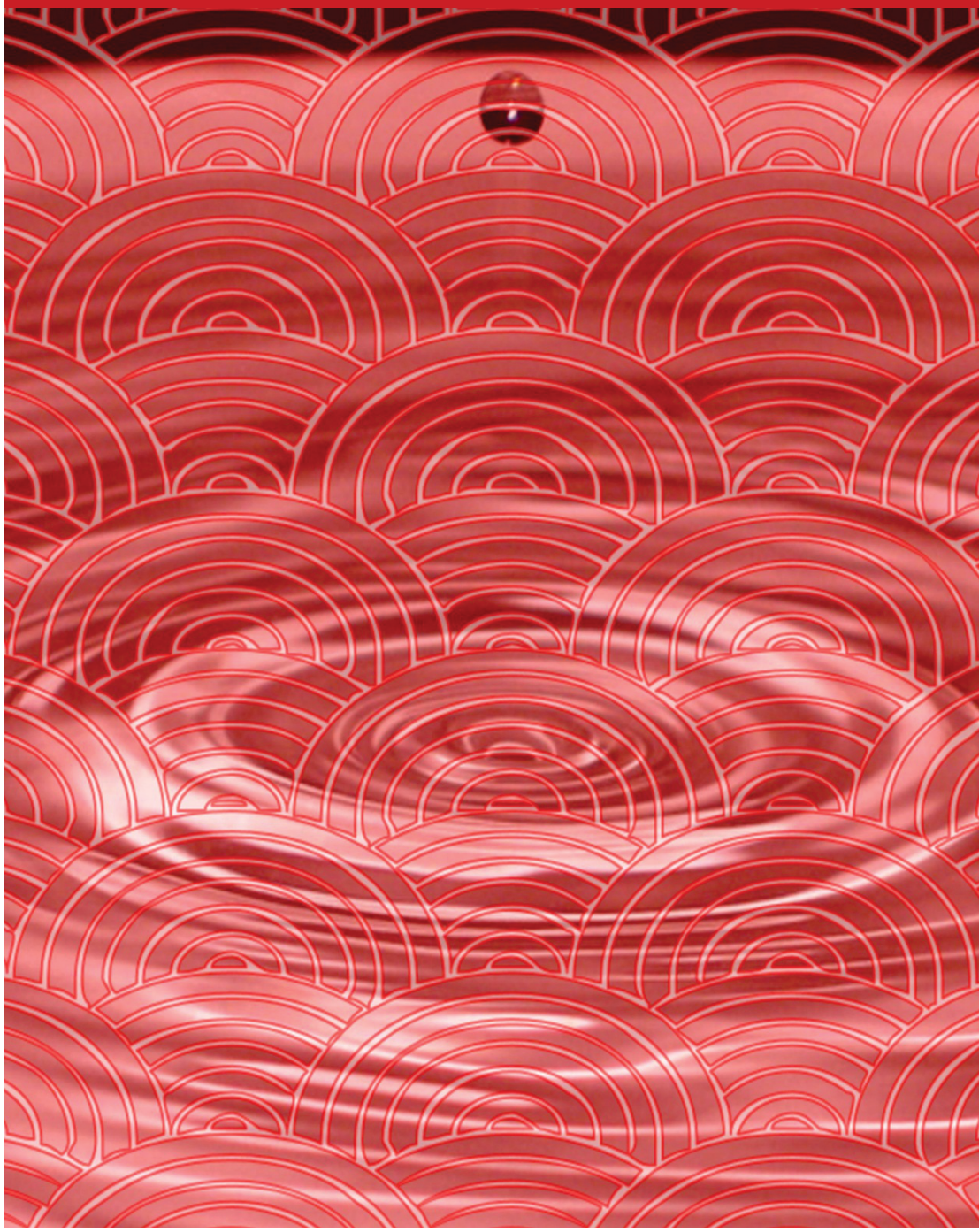

GeoPatterns

University of Bucharest

Center for Risk Studies, Spatial Modelling, Terrestrial and Coastal System Dynamics

EDITURA UNIVERSITĂȚII DIN BUCUREȘTI
BUCHAREST UNIVERSITY PRESS

GeoPatterns

EDITORIAL STAFF

University of Bucharest

Center for Risk Studies, Spatial Modelling,
Terrestrial and Coastal System Dynamics

GeoPatterns

Volume 7, 2022

EDITURA UNIVERSITĂȚII DIN BUCUREȘTI
BUCHAREST UNIVERSITY PRESS

2022

EDITURA UNIVERSITĂȚII DIN BUCUREȘTI
BUCHAREST UNIVERSITY PRESS

Editura Universității din București – Bucharest University Press
folosește sistemul de peer review dublu anonim.

Desktop Publishing: Meri POGONARIU

ISSN 2501-7837
ISSN-L 2501-7837

https://editura-unibuc.ro/

B-dul Mihail Kogălniceanu 36-46, Cămin A, Corp A, Intrarea A, etaj 2, Sector 5,
București, România (curtea Facultății de Drept)
e-mail, tel.: editura@g.unibuc.ro; + (4) 0726 390 815
Librărie online: https://editura-unibuc.ro/magazin/
Centru de vânzare: Bd. Regina Elisabeta, nr. 4-12, București, tel. + (4) 021 305 37 03

Summary

Geodynamical comparative study regarding the salt domes of two different depositional environments: Mexico and Romania

José Jorge CARACHEO-GONZÁLEZ, Marina MANEA, Vlad MANEA, Iuliana ARMAŞ 6

Four Decades of Spatial-Temporal analysis of Seismicity Patterns in the Pinotepa Nacional region, Oaxaca, Mexico

Fidel MARTÍNEZ-GARCÍA 21

Flood hazard and vulnerability-related research in Romania. The Gordian knot of conceptual and operational overlapping

Andra-Cosmina ALBULESCU 34

Exploring Risk Perception in th Romanian Covid-19 Pandemic

Daniela DOBRE, Iuliana ARMAS 45

GeoPatterns, Vol. VII (2022), pp. 6-20, https://doi.org/10.5719/GeoP.7/1

Geodynamical comparative study regarding the salt domes of two different depositional environments: Mexico and Romania

JOSÉ JORGE CARACHEO-GONZÁLEZ[1], MARINA MANEA[2], VLAD CONSTANTIN MANEA[2], IULIANA ARMAȘ[3]

[1]Faculty of engineering, UNAM, Mexico City, Mexico, [2]Computational Geodynamics Laboratory, Center of Geosciences (CGEO), UNAM, Campus Juriquilla, Queretaro, Mexico,
[3]Faculty of geography, University of Bucharest, Bucharest, Romania
jjcaracheo@gmail.com, marina@geociencias.unam.mx, vlad@geociencias.unam.mx, iulia_armas@geo.unibuc.ro

Abstract: Salt diapirs are geological formations that appear in the subsurface and are formed over millions of years. Such formations occur due to the density difference between the salt and the surrounding rock. The density difference causes the salt to penetrate throughout the strata and, therefore, the salt rises to the surface in a process known as diapirism.
The importance of salt domes, structures that form because of diapirism, lies on the fact that due to the impermeability of the salt and the deformation associated with the ascent of these structures, salt domes become excellent oil traps, with important reserves. Therefore, it is important to know the conditions that dominate the development of salt domes as well as their evolution and formation environments.
If the subsurface is considered as a continuum and by means of the momentum equations, Newton's second law and the heat conservation equation, in addition to an Eulerian approach to matter, numerical models showing the evolution of salt domes can be created, and thanks to them, the parameters that influence the formation of the domes can be calculated.
In this work it is concluded that some of the parameters that determine the formation and ascent of the diapir are the width and height of the initial Gaussian anomaly, the viscosity of the salt, the temperature, and the thickness of the salt layer.

Keywords: Diapirism, Prahova, Subcarpathians, Romania, Mexico.

1. INTRODUCTION

Various salt structures including slat diapirs represent an important economic interest, both for their nature as sources of salt for industrial use, as well as the relationship of these structures with other resources, specifically hydrocarbons, whose importance is indisputable. Salt diapirs are a mass of salt, which flows with a ductile behavior (from a geological standpoint) in discordance with the overburden (Jackson & Hudec, 2017a; Mrazec, 1907; J. Warren, 1999). Both in Mexico and Romania there are important oil and gas resources related to these structures; some of the most important hydrocarbon provinces in the world are located on salt basins, for example the Gulf of Mexico, the Persian Gulf, the North Sea, the lower Congo basin and the Precaspian Basin (Jackson & Hudec, 2017c; J. Warren, 1999; Tămaș, 2018).

2. AIMS AND OBJECTIVES

The main objective of this paper is to compare two large salt deposit provinces where it is possible to observe the phenomenon of salt tectonics in the form of salt domes and salt diapirs. The salt basins where the study was performed are *"La Popa"* basin located in the north of Mexico and the eastern Carpathian bend zone in Romania. This comparative study aims to contribute to the search for a better understanding of the geodynamical behavior (spatial and temporal evolution) of salt diapirs. To accomplish this task numerical tools are used to analyze the geodynamic evolution of salt domes in both regions.

3. ABOUT SALT DOMES AND SALT DIAPIRS

In addition to the evidence provided by the salt diapirs on the plastic behavior of rocks, salt diapirs

are of great importance in structural geology. These geological structures can have different shapes because of the previous formation of a diapir. In general, salt diapirs are formed by the buoyancy force generated by the difference in salt densities when salt is buried beneath more types of sediments (Figure 1). Because of its low density compared to adjacent rocks and overburden, salt tends to flow upward, thereby forming domes (i.e., the structure formed by the uplift of a salt core and its covering of deformed layers, Harris & Veatch, 1899) layers, pillars, and other structures (Figure 2).

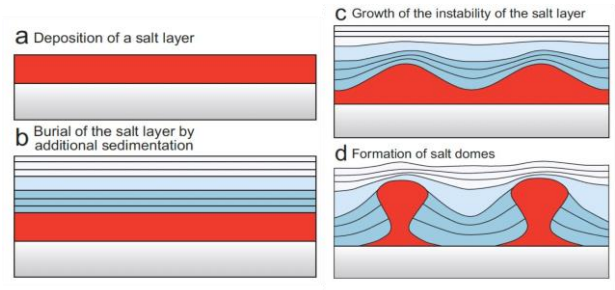

Figure 1. *Phases of the formation of a salt diapir*

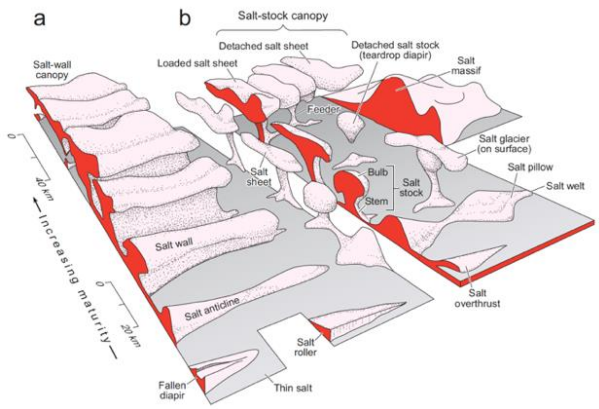

Figure 2. *Common structures in salt diapirs (M. P. A. Jackson & Talbot, 1986)*

Usually in tectonically unactive areas, the rise of salt domes occurs only at the surface due to the density difference (downbuilding), since the density of salt is approximately 2.2 g/cm3, which makes it less dense than the overlying rocks (2.5-2.7 g/cm3) (Jackson & Hudec, 2017c). However, due to tectonic movements, the salt mass can flow along faults and produce a great diversity of different types of structures. The saline basins where diapirism takes place in Mexico are: The "*Salina del Istmo*" basin, The "*La Popa*" basin and the "*El Perdido*" Folded Belt, as well as the Eastern Carpathian bend zone in Romania. It is worth mentioning that Romania is the first country in the world that has developed the exploitation of hydrocarbons associated to saline formations (Jackson & Hudec, 2017c).

By the end of the 18th century, oil exploitation began in the Câmpina region (Romania) on an industrial scale. Romania extracted 275 tons in the year of 1857 only (Vassiliou, 2018). It is worth mentioning that oil extraction in this area dates to the times of the Roman Empire. Likewise, in the year of 1646, oil was already extracted from shallow wells (*Istoria Romaniei*, 1960). In the year 1856 the first oil refinery in the world was built, precisely in the city of Ploiesti, Romania; followed by the largest and most modern oil refinery in Europe, built in the city of Câmpina, also in Romania (Vassiliou, 2018). The fact that Romania was the first country to extract oil is not a coincidence, since probably, Romania possesses one of the largest salt reserves in Europe (Maftei et al., 2009).

It is known that a significant percentage of the world's oil production comes from salt-cored structures, which caused the folding of younger stratigraphic units without intrusion. In addition to oil and gas, most of the world's sulfur, salt and potassium production comes from these types of deposits (Jackson & Hudec, 2017c).

4. HISTORICAL BACKGROUND

In Romania, oil fields are related to the Gura Ocniței – Moreni – Florești – Băicoi – Țintea diapir alignment. These areas have a production history of more than 140 years (Tămaș, 2018) (Figure 3).

The Eastern Carpathian bend zone is an area that has been heavily influenced by salt tectonics. The term salt diapirism was first proposed by the Romanian geologist Ludovic Mrazec (Figure 4) at the third international petroleum conference in 1947 (Tămaș, 2018).

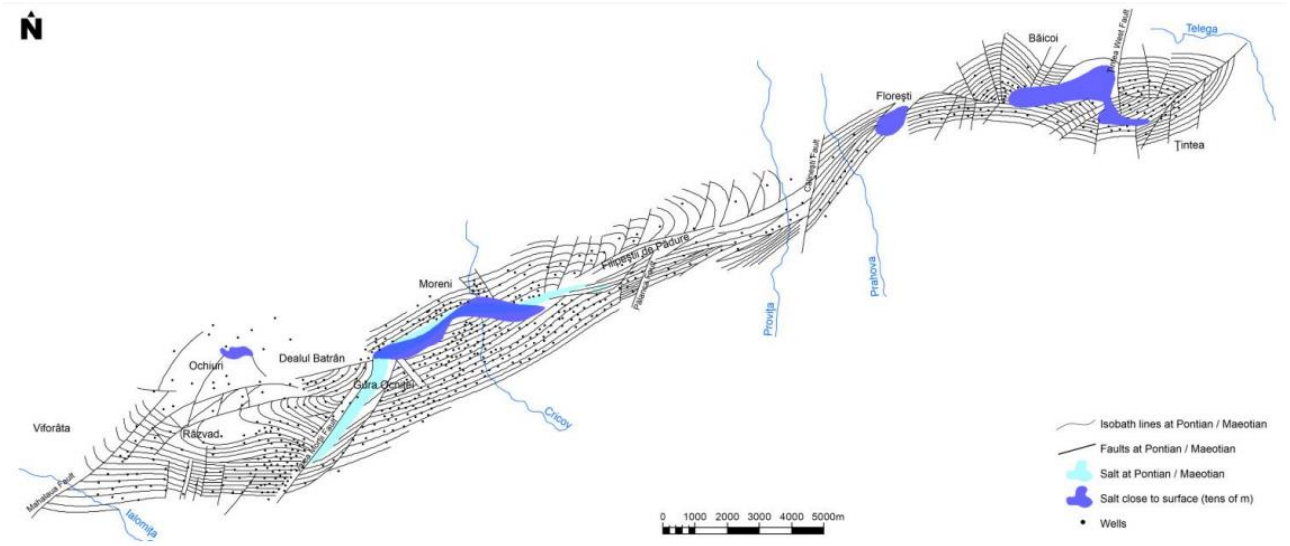

Figure 3. *Diapir alignment in Romania. After Tămaș (2018)*

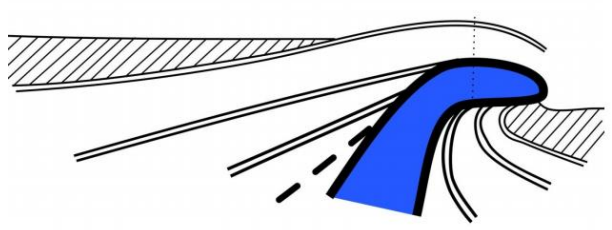

Figure 4*. Moren diapir schematics, modified from Mrazec. After Tămaș et al. (2015)*

On the other hand, the relationship between salt domes and oil was almost unknown in the United States and Mexico until the discovery of the Spindletop Hill Texas oil field in January 1901 (*How Salt Domes Were Created | Magna Resources Management Corporation*, n.d.). An independent oil prospector and amateur geologist named Patillo Higgins, from Texas, took his Sunday class to a small hill located on level ground and which had a sulfur smell. To amuse his students, Higgins would embed an empty stick in the ground and gas would come out through it, which when ignited caused a flame. This planted the idea in Higgins of the existence of an oil field in the area. After convincing Captain Anthony Francis Lucas, an Austro-Hungarian engineer from modern-day Croatia and naturalized American, both began to drill in the area. On January 10, 1901, after drilling to a depth of 347 m, the well exhaled a gusher more than 50 m high (Figure 5), which aroused great interest in the exploration of similar reservoirs on the Gulf coast (Halbouty, 2002). In Mexico, salt deposits are known to exist in several regions of the country, such as Chihuahua, Nuevo León and the southeast: Tabasco, Chiapas, Campeche, and Veracruz. However, the salt deposits in the north of the Isthmus of Tehuantepec, located in the southeast of the country, are the most economically important, as well as the best studied. Their discovery dates to the beginning of the 20th century, during the oil exploration works carried out in the Jáltipan-Potrerillos region, Veracruz, between 1902 and 1906 (Benavides García, 1983).

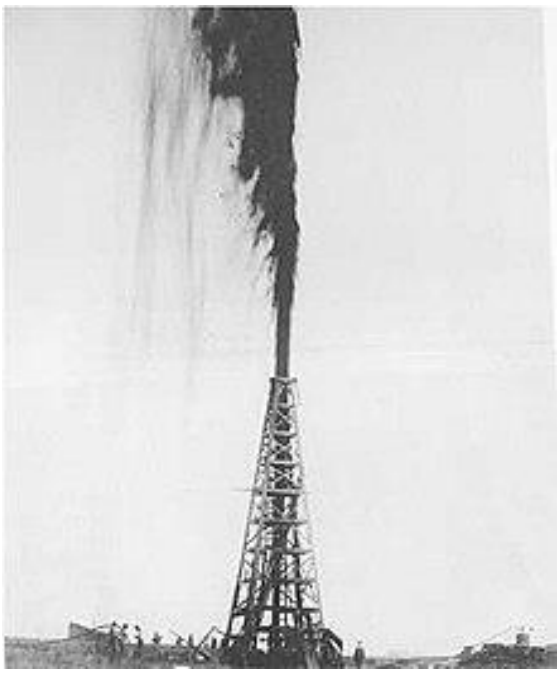

Figure 5. *Lucas gusher from in spindletop Texas, 1901, after Wikimedia commons, 2008*

5. SALT BASINS IN THE WORLD AND THEIR DEPOSITIONAL ENVIRONMENTS

Large salt diapirs and allochthonous salt layers can only be formed from a thick source layer rich in halite (NaCl). When such source layers do not have a hyperbolic shape, they are known as salt giants, mega evaporites or also as mega halites, due to large extensions such as the Louann salt (Minas Viejas Formation, northern Mexico) from the Jurassic, deposited prior to the opening of the Gulf of Mexico (e.g., Hudec et al., 2013). However, there are no modern analogs to these formations. Currently, the largest salt basin in formation is the Salar de Uyuni (Figure 6), which is located at 3,660 m above sea level in the Bolivian Andes. Despite its large size, this basin does not compare to the size of the largest ancient evaporite basins that were fed by seawater (Jackson and Hudec, 2017a).

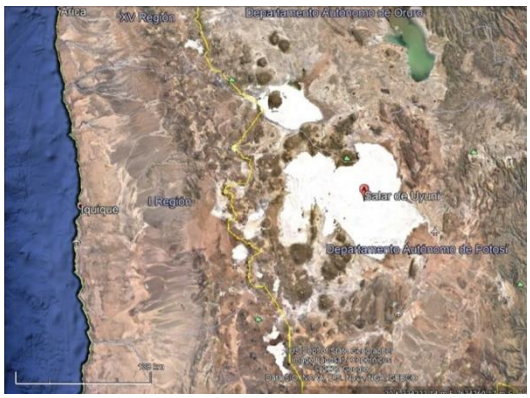

Figure 6. *Location of salar de Uyuni located in the andinian region of Bolivia, the white spots in the image above represent an evaporite extention of aproximately 10 085 km^2. Image taken from Google Earth (2020)*

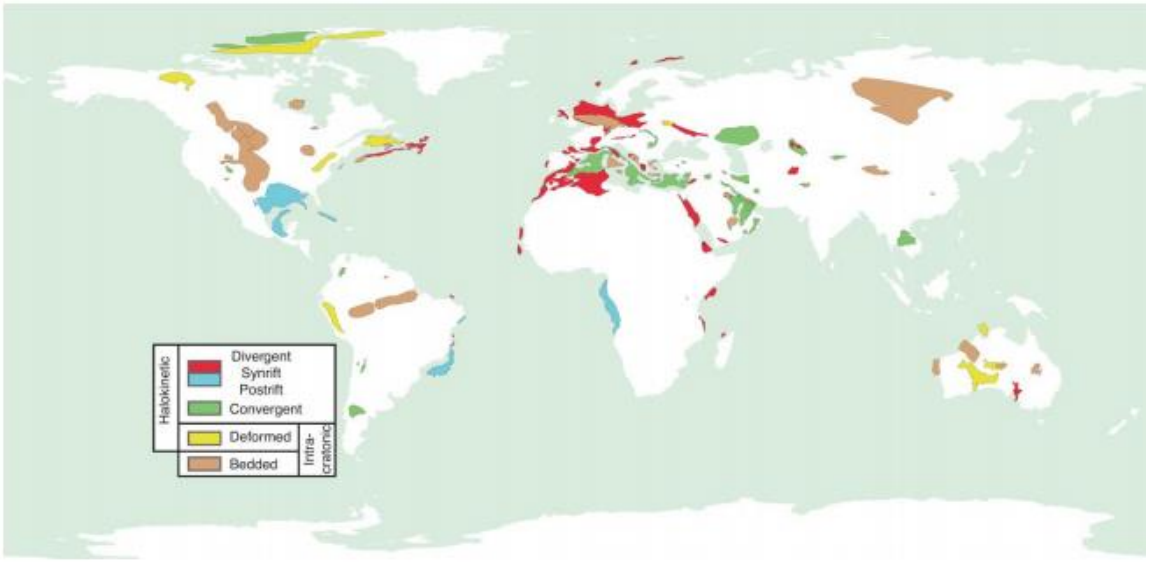

Figure 7*. Clasification of the main evaporite basins (mainly NaCl) Clasificación de cuencas de evaporitas (principalmente de NaCl) located under a context of tectonic environments. After Warren (2010)*

These systems were common in regions whose marine water evaporation rate was at its maximum level, such regions were in the past equivalent of today's "horse latitudes" (Figure 8) (J. K. Warren, 2010), also known as high subtropical. Such latitudes are found around 30° north and south of the equator and are characterized by calm winds, low precipitation, and sunny skies (NOAA, n.d.). However, much like present-day evaporites of non-marine origin, the emplacement of Phanerozoic marine evaporites in areas of suitable aridity expanded into the equatorial belts (J. K. Warren, 2010).

The reason for the absence of large salt bodies at present-day time is due to two main reasons, the tectonic setting and the long-lasting paleoclimatic changes known as icehouse-greenhouse-hothouse supercycles (Jackson and Hudec, 2017a). Greenhouse and hothouse conditions favor the precipitation of mega halites, as the warmth makes higher salinity possible, and the seas have only slight fluctuations, which allow a constant salinity level to be maintained under modern-day icehouse conditions. The ice caps cause conditions to be highly variable for a large accumulation of evaporites to take place (Jackson and Hudec, 2017a).

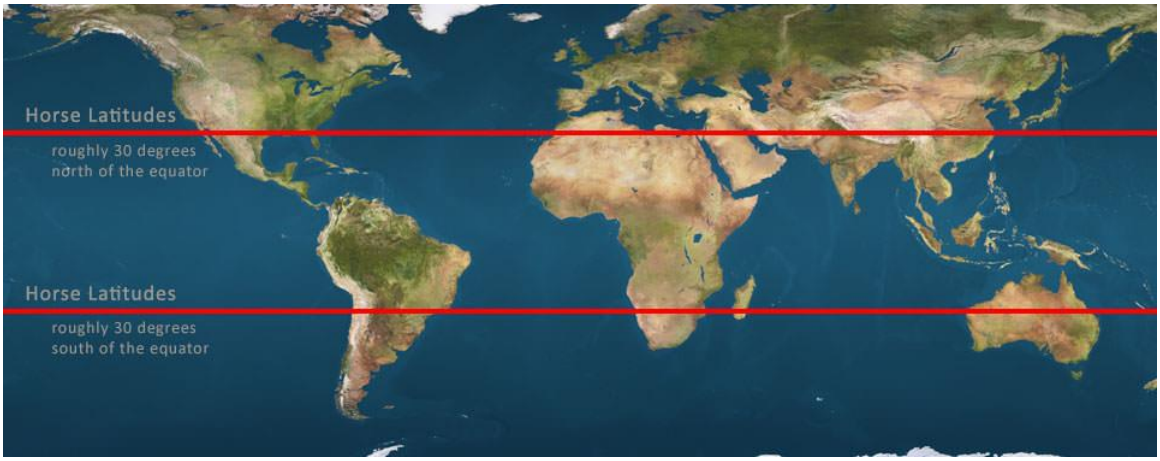

***Figure 8**. Horse Latitudes, after NOAA, n.d.*

The second reason is that the hydrographically isolated conditions required to form evaporites are best developed within large basins when supercontinent breakup or accretion occurs (Jackson and Hudec, 2017a). Continental collisions create hydrographically isolated forearc basins. This is the case of the La Popa basin in Mexico (Figure 9) and the Muntenian Carpathians in Romania (Figure 10), whereas when a supercontinent breaks apart the rifting process creates hydrologically isolated rifts or shallow ocean basins, for example, in the Gulf of Mexico and the South Atlantic (Jackson & Hudec, 2017a).

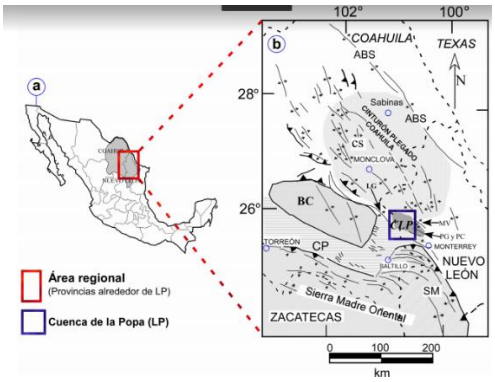

***Figure 9.** La Popa basin, located between the states of Nuevo León and Coahuila. After Tamez-Ponce et al. (2011)*

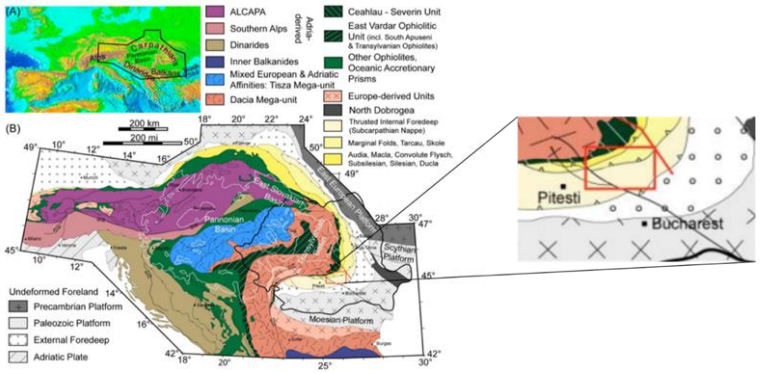

***Figure 10**. Map of the Alpine, Carpathian and Dinaric mountains. Geological arrangement of the Romanian Carpathians, the red box encloses the study area, the diapir fold zone (DFZ) (modified from Tămaș, 2018)*

6. STUDY AREAS

The Carpathian Mountains

As can be seen in Figure 10, the Carpathian Mountains are an eastern extension of the European Alps fold-thrust belt (Krézsek and Bally, 2006). The study area is located 100 km north from Bucharest. The Carpathians Mountains were formed due to the colliding of the African plate against the European plate in an event known as the Alpine orogeny which led to the formation of several basins systems on top of the Eo-alpine structures (Krézsek and Bally, 2006).

The first colliding took place during the late Jurassic, as consequence nappe systems were created during the middle cretacic, (Frisch et al., 2010), the strong bending on the area is characteristic of the Carpathians and there are two main salt horizons (Figure 11), both dating to the Miocene, the early Burdigalian and the Middle Serravallian. The evaporites where first deposited on the Carpathians foreland and later over the nappes. The salt formation studied on this paper is of Burdigalian age.

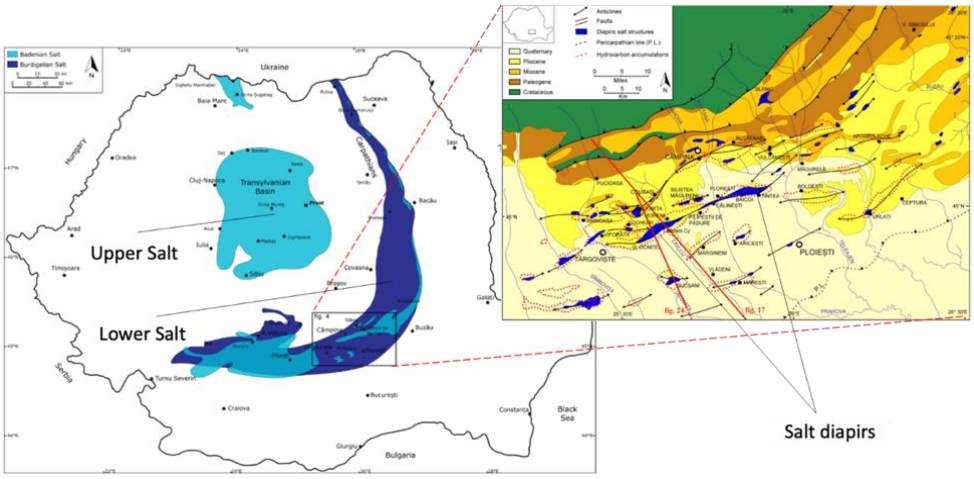

Figure 11. *Map of the lower and upper salt formations, on the zoomed area the salt diapirs present on the area can be. Modified from Tămaș (2018)*

The late deformation phase of the region is related to compression within the plate accommodated by thick-skinned deformation, (Wallachian phase), (Hippolyte and Sandulescu, 1996). The Diapirs Fold Zone (DFZ) sedimentary column comprises over 4 km thick Cretaceous to Middle Miocene clastic deposits overlying a thin succession of Middle Miocene evaporites and shales. The Cretaceous to Middle Miocene section has been locally covered by more than 2 km of Late Miocene to Quaternary shallow marine and fluvial sediments (Figure 12 and Table 1) (Tămaș, 2018).

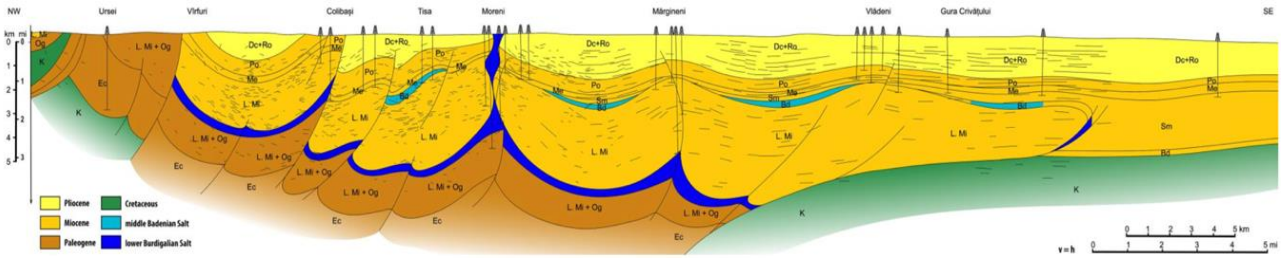

Figure 12. *NW-SE simplified geological section through the Moreni diapir, where the local stratigraphy is shown, K=Cretaceous, Eo= Eocene, Oc=Oligocene, L.Mi=Early Miocene, Bd=Badenian, Sm-Sarmacian, Me=Maeocene, Po=Pontianian, Dc=Dacian, Ro=Romanian. Taken from Tămaș (2018)*

"La Popa" *Basin*

The other study area encompassed in this study is *"La Popa" a* foreland pull apart type basin located in the northern part of Mexico, 85 km away the city of Monterrey, this basin is located over the front part of the eastern *Sierra Madre* (ESM) in that basin there are gypsum deposits representing eroded salt reserves, a 25 km fault- shape structure can be identified in blue on the image below, indeed, that structure is a salt weld (Figure 13).

La Popa basin is Linked to the opening of the Gulf of Mexico (200 Ma) with Callovian salt (163 Ma) (Minas Viejas/Sal Louann Formation). The formation of the basin can be described in 4 phases, Figure (14):

a) Opening of the Gulf of Mexico, displacement of the Yucatan block, deposition of Callovian salt.
b) End of salt deposition.
c) Creation of oceanic floor during the Tithonian.
d) Actual disposition of the Gulf of Mexico.

The salt tectonics in *"La Popa"* basin have been influenced by the formation of WSM formation during the late Cretaceous up the early Paleogene (70-50 Ma). The salt of Callovian age is called the "*minas Viejas*" formation in Mexican literature and Louann salt in American literature, is overlaid by a late Cretaceous to Middle Eocene siliciclastic succession deposited during the uprising of the WSM (70 Ma-45 Ma) and the Zuloaga formation of marine limestones of middle Jurassic to late

cretaceous age (Figure 15 and Table 1), which covers the surface, (Lawton et al., 2001). The initial thickness of the salt is estimated in 2,100 m of halite, followed by 520 m of carbonate black limestone and halite intercalation and a basal interval of carbonate black limestone of 370 m, (Lopez-Ramos, 1982).

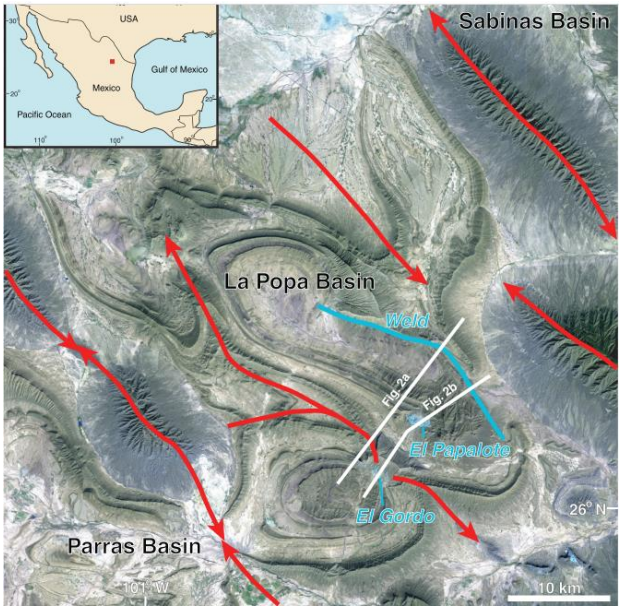

Figure 13 The *"El Gordo"* and *"El Papalote"* diapirs *and "La Popa" salt weld of 25 km of extensions (blue). Axial traces of detachment folds of the Mexican orogeny (red). After Rowan et al. (2003)*

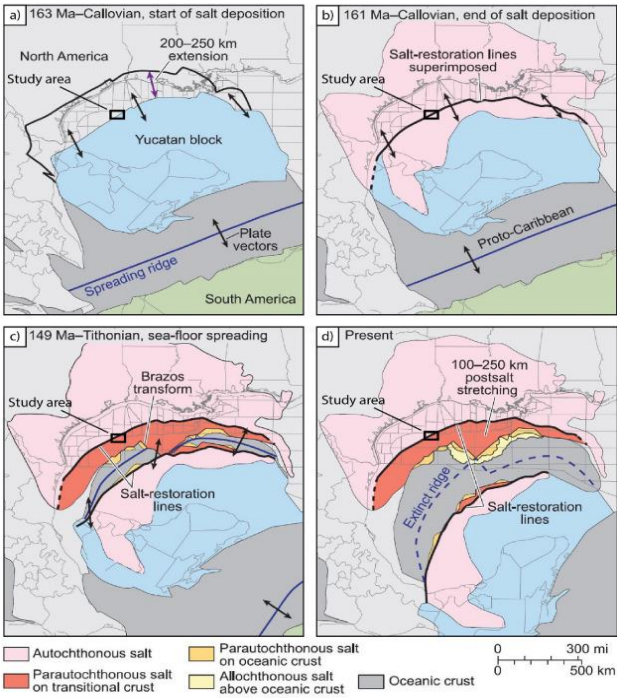

Figure 14 *Paleogeographic reconstruction of the Gulf of Mexico, a) beginning of the opening of the Gulf with the displacement of the Yucatan block and therefore, the beginning of Callovian salt deposition; b) end of salt deposition; c) creation of the ocean floor during the Tithonian; d) Actual disposition of the Gulf of Mexico. After Roelofse et al. (2020)*

Table 1. Comparison between the stratigraphy of both basins the Carpathians (right) and La Popa (left). In red the evaporite formations are shown and in blue the same ages in both basins, the salt in La Popa basin its older than the salt in the Carpathians. Modified from Vega and Lawton (2011)

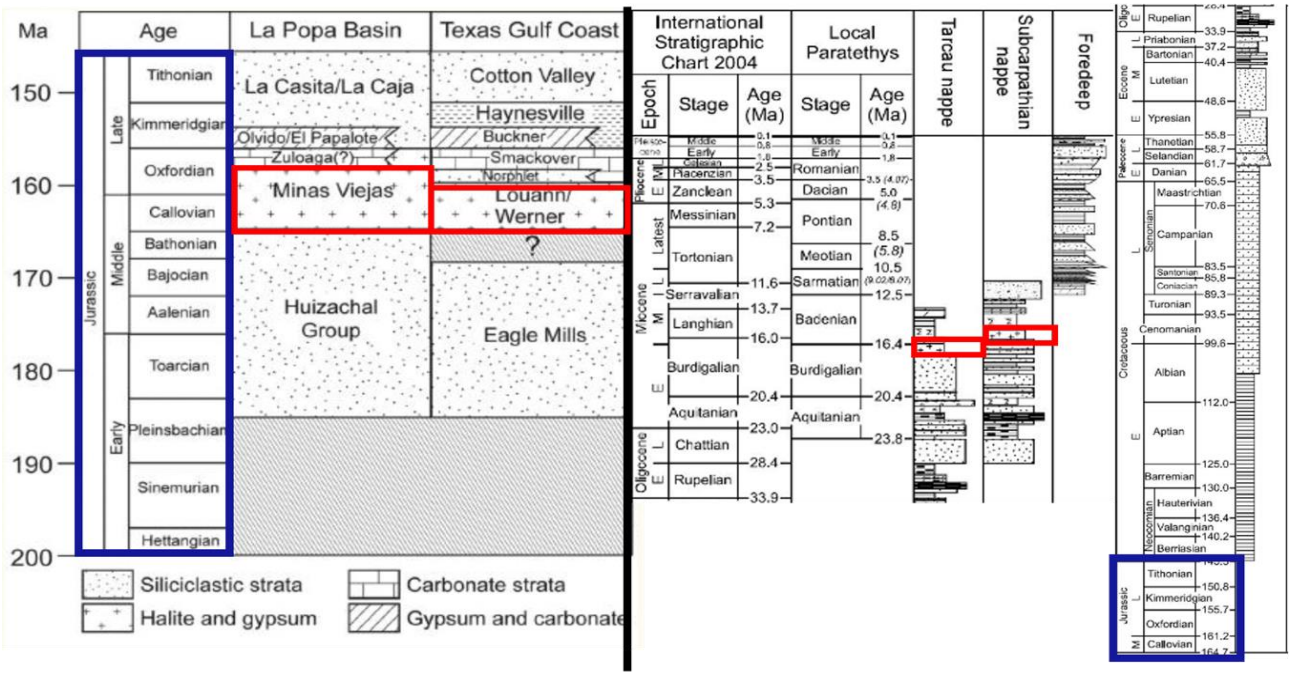

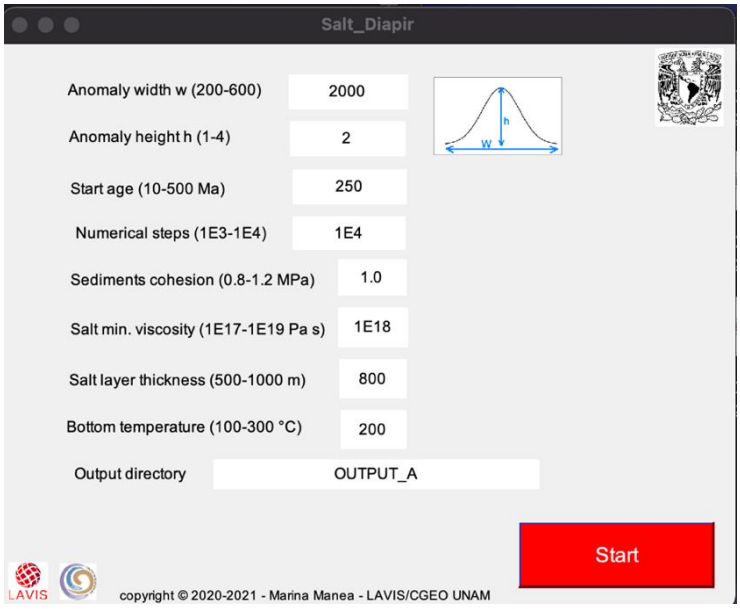

Figure 15. *Interface of the Salt_diapir v 1.0 with the parameters displayed*

7. METHOD AND RESULTS

Since salt diapirs represent an important part of the world's hydrocarbon reserves it is of great importance to understand the evolution of salt basins and diapirs, as well as their causes and occurrence. For this, it is necessary to carry out studies where the evolution of different basins is compared. Numerical tools were used to study the evolution of salt diapirs under different conditions.

To simulate the evolution of the salt diapirs the software Salt_Diapir v1.0 created at the national laboratory of advanced scientific visualization of the National Autonomous University of Mexico (LAVIS UNAM, by its initials in Spanish) was used.

The software performs numerical simulations under the following considerations: Linear temperature distribution along with the depth, typical rheological behavior of halite, no tectonical deformation is considered in the simulations, an initial salt anomaly in the form of a Gaussian bell (From now on referred to as Gaussian anomaly), density difference between the salt layer (salt=2.1 g/cm3) and sediments (sediments=2.7 g/cm3). Interface of the software is show in the image below (figure 16).

a) Anomaly width w = indicates the horizontal extent of the Gaussian anomaly,
b) Anomaly height = indicates the vertical extent of the Gaussian anomaly,
c) Start age = indicates the time it takes for the diapir to surface,
d) Numerical steps = indicates the number of iterations the program performs to simulate the diapir,
e) Sediments cohesion = indicates the cohesion of the sediments overlying the salt layer,
f) Salt min. Viscosity = indicates the viscosity of the salt layer,
g) Salt layer thickness = indicates the thickness of the salt layer,
h) Bottom temperature = indicates the temperature of the salt layer.

To better understand how the rising of salt diapirs is affected by different parameters, 26 simulations of salt diapirs were performed on the software Salt_Diapir v1.0. The aim of these simulations was to observe how the parameters (viscosity, temperature, salt layer thickness and dimensions of the gaussian anomaly) affect the time that takes a salt diapir to reach the surface. The simulations 1 to 9 show the modifications over the dimensions (height and width) of the gaussian anomaly and the effects that this parameter has on the evolution of the salt diapir (salt layer thickness, temperature and viscosity were kept constant). Simulations 10-13 show the effects of the

temperature and its effects on the evolution of salt diapirs. For these simulations the salt layer thickness, viscosity and the dimensions height and width of the gaussian anomaly were kept constant. Simulations 14-18 depict the modifications on the salt layer thickness and its influence on the evolution and rising on the salt diapir. For these simulations the viscosity, temperature, and dimensions of the gaussian anomaly were kept constant. For the simulations 19-26, the viscosity of the salt layer is modified in a range between $1x10^{17}$ to $1x10^{19}$ Pa s, while the temperature, salt layer thickness and gaussian anomaly dimensions were kept constant (figure 16 and table 2).

Table 2. Simulation conditions

Simulation number	Salt. Min viscosity [Pa s]	Bottom temperature [ºC]	Start age [Ma] (time it takes for the diapir to reach the surface)	Salt layer thickness [m]	width [km]	heigth [km]	h/w
1	1.00E+18	200	610	800	2	2	1
2	1.00E+18	200	293	800	2	5	2.5
3	1.00E+18	200	116	800	2	10	5
4	1.00E+18	200	380	800	1	2	2
5	1.00E+18	200	139	800	1	5	5
6	1.00E+18	200	22	800	1	10	10
7	1.00E+18	200	257	800	0.5	2	4
8	1.00E+18	200	37	800	0.5	5	10
9	1.00E+18	200	4	800	0.5	10	20
10	1.00E+18	150	140	800	1000	5	-
11	1.00E+18	175	137	800	1000	5	-
12	1.00E+18	225	139	800	1000	5	-
13	1.00E+18	250	138	800	1000	5	-
14	1.00E+18	200	826	500	1000	5	-
15	1.00E+18	200	750	600	1000	5	-
16	1.00E+18	200	180	700	1000	5	-
17	1.00E+18	200	136	900	1000	5	-
18	1.00E+18	200	129	1000	1000	5	-
19	1.00E+17	200	129	800	1000	5	-
20	2.50E+17	200	132	800	1000	5	-
21	5.00E+17	200	136	800	1000	5	-
22	7.50E+17	200	136	800	1000	5	-
23	2.50E+18	200	142	800	1000	5	-
24	5.00E+18	200	151	800	1000	5	-
25	7.50E+18	200	159	800	1000	5	-
26	1.00E+19	200	165	800	1000	5	

Graph 1 (in figure 16) shows the relationship between time and ascension of the diapir when viscosity of the salt layer and the rest of the parameters are kept constant. As can be seen, the higher the viscosity is, the longer the ascension time. The upward trend line and the equation of the straight line obtained can also be observed, the equation establishes diapir's ascension time as a function of salt viscosity l to $T = 3 \times 10^{-18x} + 132.28$ where T is the ascension time and x is the viscosity of the salt layer.

Graph 2 (in figure 16) shows the relationship between the thickness of the salt layer versus the time it takes to the diapir to reach the surface, and the rest of the parameters are kept constant, it is observed that the thicker the salt layer is, the shorter the ascension time. It can also be concluded that the behavior of the function is different when the salt layer thickness is smaller than 600 m, therefore, two equations were obtained, one for a thickness smaller than 600 m (blue) and another for a thickness bigger than 600 m (orange). Therefore, for a thickness

bigger than 600 m: $T = -0.76x + 1206$ where T is the ascension time and x is the salt layer thickness. For a thickness bigger than 600 m we have the following equation $T = -0.1771x + 301.86$ where T is the diapir ascent time and x is the thickness of the salt layer.

Graph 3 (in figure 16) shows the relationship between diapir's bottom temperature versus ascension time, with all other parameters kept constant, unlike the other parameters, the relationship between temperature and time is not proportional and, after the Salt_Diapir v 1.0 software, temperature does not play a very important role in the diapir's ascension to the surface.

Graph 4 (in figure 16) shows that while the anomaly height (h), at constant parameters, is bigger than its width (w), the ascent time also decreases, this is very clearly observed in model M9, where the formation time is only 4 Ma. An exponential equation was also obtained, this equation establishes that $T = 575.33e^{-0.266x}$ where T is the ascent time and x is the height over width ratio of the anomaly.

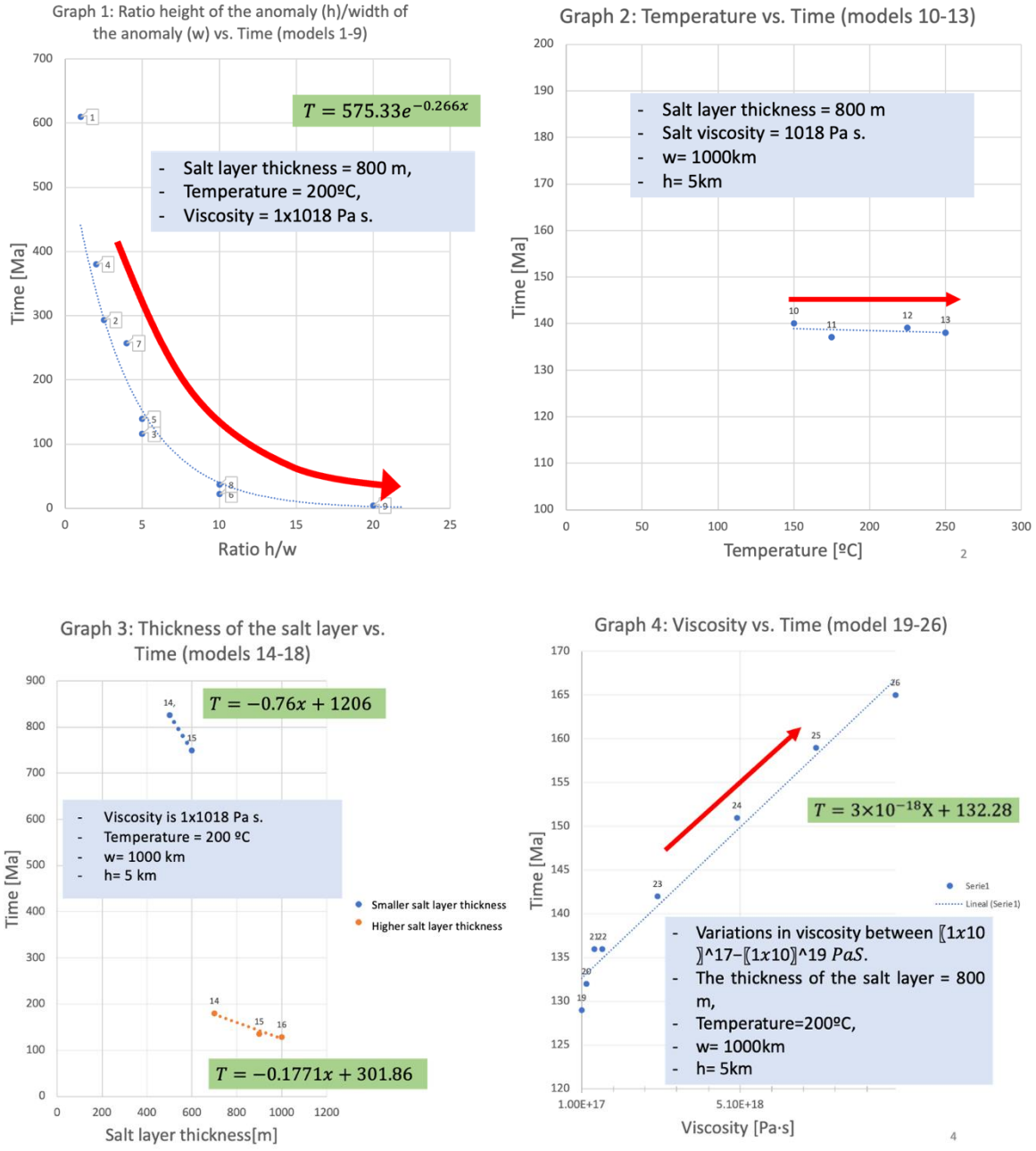

Figure 16. *Simulation results. The number above the dots on the graphs indicates the model number. Parameters are Viscosity [Pa s], temperature [ºC], salt layer thickness [m], time [Ma], Gaussian anomaly base width (w) [km] and Gaussian anomaly height (h) [km].*

8. REGIONAL DIFERENCE AND FUTURE DIRECTIONS

According to the geological history of both basins, the processes that took place are similar, both are foreland basins and were affected by compressional tectonic events, such as the Alpine orogeny and the Mexican orogeny, which gave origin to the Carpathian Mountains and the eastern Sierra Madre respectively. From the above it can be deduced that the diapirs present in both basins have been affected by tectonic shortening.

Both in the La Popa and Carpathians sedimentary environments there were periods of passive diapirism, due to sediment deposition on the salt ("downbuilding"), as well as active diapirism due to compressional shortening events that affected it. The main difference between both basins lies on the salt's age of deposition; the salt present in the La Popa Basin dates to the Jurassic, more specifically to the Bajocian-Bathonian age (Pindell et al., 2021), whereas the salt in the Carpathians is much more younger since there are Miocene salt formations, specifically from Burdigalian and Serravallian ages (Tămaș, 2018). Likewise, the salt layer thickness is thicker in the La Popa basin than it is in the Carpathians. The thickness of the La Popa salt layer is greater than 2 km (Vega and Lawton, 2011) whilst the salt layer thickness in the Carpathians its approximately 1.5 km (Tămaș, 2018).

On the simulations carried out with the Salt_Diapir v 1.0 software (Figures 17 and 18), it can be observed that the horizontal extension of the Carpathians diapir its smaller than the one in the La Popa basin diapir. This is due to the difference between the thickness of the salt in both basins. Likewise in both basins a detachment is observed. It is also evident that the salt weld is narrower in the Carpathians, which indicates the importance of the salt thickness in the development of the diapir. Another aspect of the rising of a salt diapir is the importance that the age of salt deposition and the compressional shortening play on the rising of a salt diapir. Despite that the salt of Miocene age in the Carpathians is younger than the Jurassic salt in the La Popa basin, both have reach to the surface, even doe the process of salt ascension piercing through the overburden takes millions of years. Whereas the rising of salt diapirs in the La Popa occurs by downbuilding processes, in the Carpathians the rising of the diapirs is "helped" by the compressional tectonic shortening of the Carpathians and acting like an extruder of the salt.

To study, the evolution and differences between the La Popa basin and the eastern Carpathian bend zone in a deeper way it is necessary to know the conditions present in both basins, e.g. the arrangement and disposition of diapirs and salt formations in each one of the basins. In addition, since the program used in this research only considers density differences during diapir development, in future works downbuilding and tectonic shortening processes should also be considered. This could help to represent the deformation processes, evolution and final configuration of salt diapirs and salt basins on a more reliable way. Differences in salt temperature should also be considered since the temperature distribution is not uniform and it directly affects salt's density and buoyancy, which in turn affects salt flow velocity, (Jackson and Hudec, 2017c).

La Popa

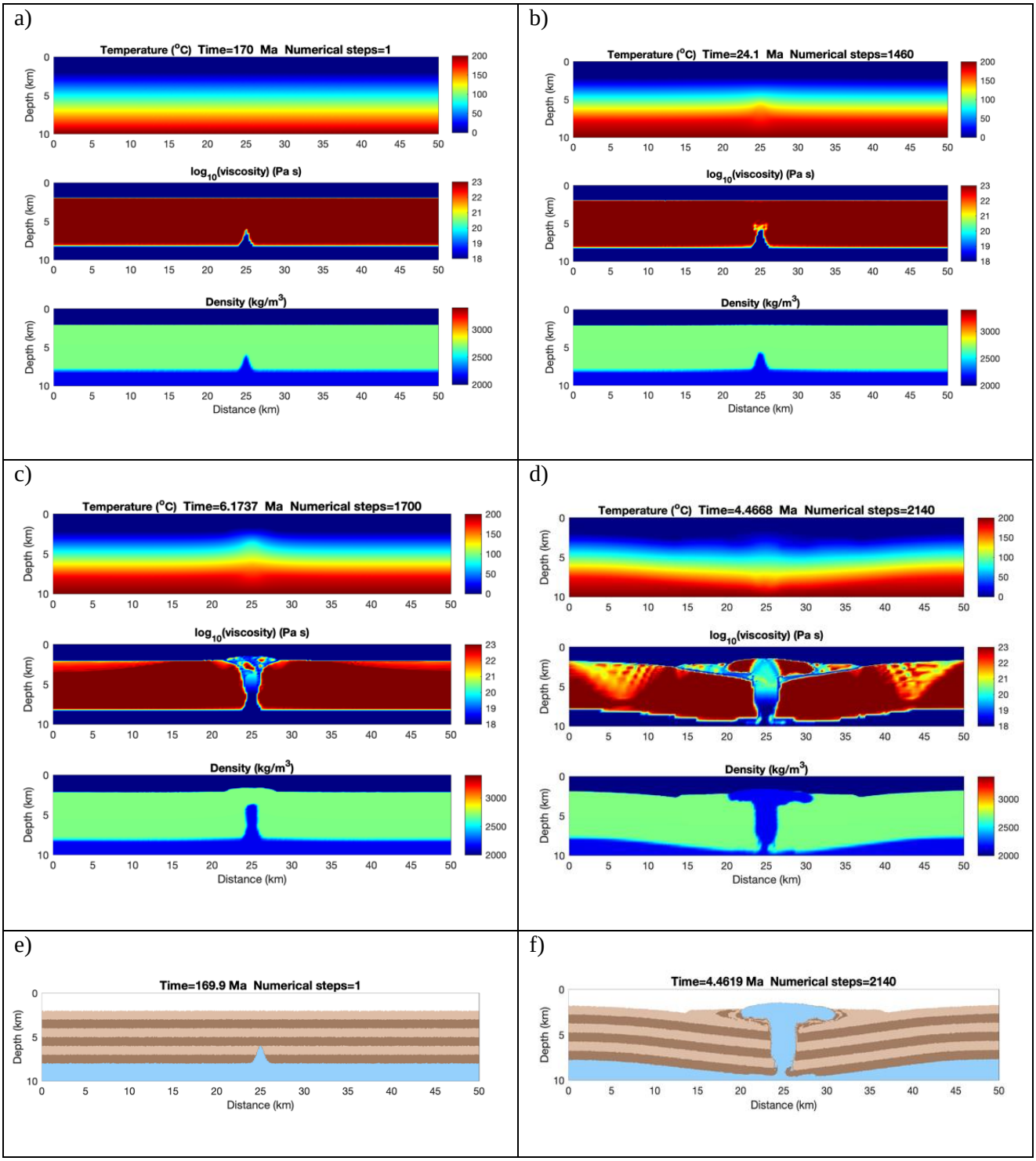

Figure 17. *Models of La Popa basin made with the salt diapir software, a) initial temperature distribution in the La Popa basin, d) final temperature distribution in the La Popa basin, e) original arrangement of the strata in La Popa, f) final disposition of the strata in La Popa caused by diapirism.*

Carpathians

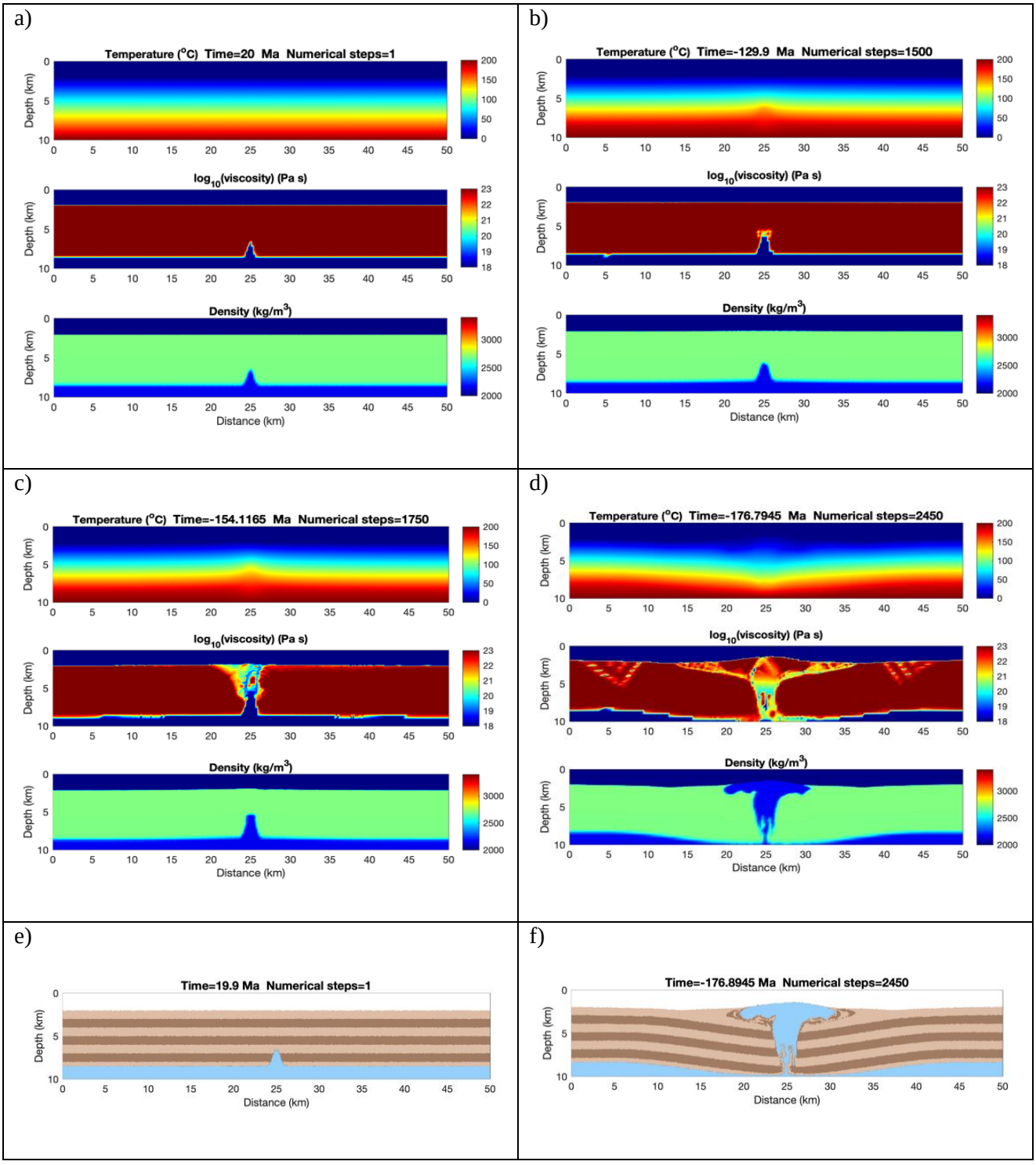

Figure 18. *Models of the Carpathians basin made with the salt diapir software, a) initial temperature distribution in the Carpathian, d) final temperature distribution in the Carpathian, e) original arrangement of the strata in the Carpathian, f) final arrangement of the strata in the Carpathians caused by diapirism.*

REFERENCES

Benavides García, L. (1983). DOMOS SALINOS DEL SURESTE DE MÉXICO Origen: Exploración: Importancia Económica. *Boletin de La Asociación Mexicana de Geólogos Petroleros*, *35*(1), 9–35.

Frisch, W., Meschede, M., & Blakey, R. C. (2010). *Plate tectonics: continental drift and mountain building*. Springer Science \& Business Media.

Halbouty M.T. (2002). Spindletop: The Original Salt Dome. *World Energy Magazine*, *3*(2), 108–112.

Harris, G. D., & Veatch, A. C. (1899). *A preliminary report on the geology of Louisiana, in Geological Survey of Louisiana report: Baton rouge*.

Hippolyte, J.-C., & Sandulescu, M. (1996). Paleostress characterization of the "Wallachian phase" in its type area (southeastern Carpathians, Romania). *Tectonophysics*, *263*(1–4), 235–248.

How Salt Domes Were Created | Magna Resources Management Corporation. (n.d.). Retrieved December 5, 2021, from http://www.magna-resources.com/history-of-salt-domes

Istoria Romaniei (Vol. 2). (1960).

Jackson, M. P. A., & Hudec, M. R. (2017a). Evaporites and Their Deposition. In *Salt Tectonics* (pp. 12–27). Cambridge University Press. https://doi.org/10.1017/9781139003988.004

Jackson, M. P. A., & Hudec, M. R. (2017b). Introduction. In *Salt Tectonics* (pp. 2–11). Cambridge University Press. https://doi.org/10.1017/9781139003988.003

Jackson, M. P. A., & Hudec, M. R. (2017c). Salt Flow. In *Salt Tectonics* (pp. 28–60). Cambridge University Press. https://doi.org/10.1017/9781139003988.005

Jackson, M. P. A., & Talbot, C. J. (1986). External shapes, strain rates, and dynamics of salt structures. *Geological Society of America Bulletin*, *97*(3), 305–323. 10.1130/0016-7606(1986)97<305:ESSRAD>2.0.CO;2

Krézsek, C., & Bally, A. W. (2006). The Transylvanian Basin (Romania) and its relation to the Carpathian fold and thrust belt: Insights in gravitational salt tectonics. *Marine and Petroleum Geology*, *23*(4), 405–442. https://doi.org/https://doi.org/10.1016/j.marpetgeo.2006.03.003

Lawton, T. F., Vega, F. J., Giles, K. A., & Rosales–Domínguez, C. (2001). Stratigraphy and Origin of the La Popa Basin, Nuevo León and Coahuila, Mexico, in Bartolini, C., Buffler, R.T., Cantu–Chapa, A. (eds.), The Western Gulf of Mexico Basin: Tectonics, sedimentary basins, and petroleum systems: Tulsa, Oklahoma, U. S. A. *American Association of Petroleum Geologists Memoir*, *75*, 219–240.

Lopez-Ramos, E. (1982). *Geología de México: Vol. II*. Consejo Nacional de Ciencia y Tecnología.

Maftei et al. (2009). New aspects concerning geoelectrical tests on shallow landslides in Telega, Romania. *EGU General Assembly 2009, Held 19-24 April, 2009 in Vienna, Austria Http://Meetings. Copernicus.Org/Egu2009*, 3397–3397.

Mrazec, L. (1907). Despre cute cu simbure de străpungere [On folds with piercing cores]. *Buletinul Societății de Științe Din București*, *16*, 6–8.

NOAA. (n.d.). *What are the horse latitudes?* National Ocean Service Website. Retrieved October 1, 2020, from https://oceanservice.noaa.gov/facts/horselatitudes.html#:~:text=The%20horse%20latitudes%20are%20regions,calm%20winds%20and%20little%20precipitation.&text=Unable%20to%20sail%20and%20resupply,ran%20out%20of%20drinking%20water

Pindell, J., Villagómez, D., Molina-Garza, R., Graham, R., & Weber, B. (2021). A revised synthesis of the rift and drift history of the gulf of mexico and surrounding regions in the light of improved age dating of the middle jurassic salt. In *Geological Society Special Publication* (Vol. 504, Issue 1, pp. 29–76). Geological Society of London. https://doi.org/10.1144/SP504-2020-43

Roelofse, C., Alves, T. M., & Gafeira, J. (2020). Structural controls on shallow fluid flow and associated pockmark fields in the East Breaks area, northern Gulf of Mexico. *Marine and Petroleum Geology*, *112*(1).

Rowan, M. G., Lawton, T. F., Giles, K. A., & Ratliff, R. A. (2003). Near-salt deformation in La Popa basin, Mexico, and the northern Gulf of Mexico: A general model for passive diapirism. *AAPG Bulletin*, *87*(5), 733–756.

Tămaș, D. M. (2018). *Salt tectonics in the Eastern Carpathian Bend Zone, Romania*. Babeș-Bolyai University.

Tămaș, D. M., Krezsek, C. & Schleder, Z. G. (2015). *3D diapir modeling in the type area for salt diapirism, preliminary results (Moreni, Romania)*. 40–49. https://doi.org/10.13140/RG.2.1.2988.9362

Tamez-Ponce, A., Yutsis, V., Krivosheya, K., Román, E., Flores, H., Bulychev, A. A., Vargas, A. T., Linares, N., & León, M. (2011). *Boletín de la Sociedad GeolóGica Mexicana VoluMen 63* (Issue 2).

Vassiliou, M. (2018). *Historical dictionary of petroleum industry* (2da edición). Lanham MD: Rowman and Littlefield-Scarecrow Press.

Vega, F. J., & Lawton, T. F. (2011). Upper Jurassic (Lower Kimmeridgian-Olvido) carbonate strata from the La Popa Basin diapirs, NE Mexico. *Boletín de La*

Sociedad Geológica Mexicana, *63*(2), 313–321. http://boletinsgm.igeolcu.unam.mx/bsgm/index.php/144-sitio/articulos/cuarta-epoca/6302/507-6302-11-vega

Warren, J. (1999). *Evaporites: Their Evolution and Economics*. Blackwell Science.

Warren, J. K. (2010). Evaporites through time: Tectonic, climatic and eustatic controls in marine and nonmarine deposits. In *Earth-Science Reviews* (Vol. 98, Issues 3–4, pp. 217–268). https://doi.org/10.1016/j.earscirev.2009.11.004

GeoPatterns, Vol. VII (2022), pp. 21-33, https://doi.org/10.5719/GeoP.7/3

Four Decades of Spatial-Temporal analysis of Seismicity Patterns in the Pinotepa Nacional region, Oaxaca, Mexico

FIDEL MARTÍNEZ-GARCÍA

Independent Research in Environmental Sciences, retired staff of the Federal Electricity Commission, Mexico
Eco599395@gmx.com

Abstract. Contributing to the knowledge of the spatial distribution patterns involved in the most seismic regions of the world is an alternative way of anticipating the destructive consequences associated with significant earthquakes (>5.5Mw). This document provides evidence of the spatial aggregation patterns that are implicated in the spatial distribution of 32,046 seismic events from 1980 to 2021 period, in the Pinotepa Nacional region, Oaxaca, Mexico (Middle America Trench) and its relationship with intense local seismic activity and indirectly with possible hidden local unknown structures, settled some kilometers below the surface. Using GIS tools, to identify spatial patterns, the Local Indicators of Spatial Association analysis (LISA) and the Space–Univariate Local Moran's Index (SULMI) were applied. The analysis revealed that 21.0% of the epicenter's spatial distribution is not random but tends to cluster toward seismicity potential zones. According to the LISA-SULMI approach applied, for each significant earthquake greater than 5.5Mw, a map of color intensities was obtained representing the degree of global spatial autocorrelation between the data. After a sequence of two significant earthquakes in 2018 (7.6 - 6.0 Mw), a hidden local tectonic feature 43 kilometers in diameter was revealed just 10 kilometers below the surface by micro-seismicity (2.0 and 2.9 Mw).

Keywords: Middle America Trench, Cocos Plate, LISA analysis, Moran's Index, spatial autocorrelation 1980-2021.

1. INTRODUCTION

Contemporary knowledge about the inner structure of the Earth all over the world, the is a consequence of the natural seismic activity studies using geophysical and Earth sciences within regions with high seismic hazards like Mexico, particularly throughout the Middle America Trench (MAT). Another source of information is handmade blast-induced seismicity and scientific prospecting to understand the lithosphere by scientific drilling (Arai, 1982). For example, the Kola Superdeep Borehole (KSDB) project or SG-3 (Carr et al., 1996). One more source has been the use of current and updated methods of seismic tomography (Bianco et al., 2019) and seismic refraction to measure the thickness of the terrestrial internal layers and discontinuities between the trenches (MAT) and the continental lithospheric plate or metropolitan areas (Montalvo Arrieta et al., 2008). Likewise, MAT seismic potential (Dominguez et al., 2016) and the connection between earthquake – faults exposed by observation of seismic waves (Julian et al., 1998).

Nevertheless, joint behavior of spatial-temporal data (patterns) of the epicenters and hypocenters recorded by seismic instrumentation have also contributed importantly to delineating and locating shapes over or within the layers of the earth, within regions of seismic belts characterized by frequent seismic activity. The best-known mega-form outlined is the Pacific Ring of Fire of which numerous trenches form a part, as is the case in the Middle America Trench (northern part, also called like Acapulco Trench) (Ducea et al., 2004).

But within these regions of high seismicity and intense volcanism caused by the subduction of plates, there are subregions where the space-time pattern could show ancient internal forms still unknown, excluding fault tectonics. Under this reasoning, the geographic position and behavior of horizontal and vertical seismic activity studied over long periods can be a useful tool to define its limits within the Earth's shallow crust.

The relative geographical position (X, Y, and Z) of a group seismic event can show hitherto unknown

internal tectonic features, which would demonstrate moreover, that the spatial distribution of data in narrow areas is not random in time and space.

Under this reference frame, the main objective of this research is to demonstrate that 42 years of seismicity data within a study area located near the coastal limits of the states of Guerrero and Oaxaca, Mexico, are not distributed randomly but are clustered horizontally and vertically in specific regions of the geographical space, outlining possibly hidden tectonic features.

1.1. Study area

The study area is located entirely within the boundaries of the Jamiltepec District and the most distinctive municipality is Santiago Pinotepa Nacional, in the state of Oaxaca, Southern Mexico. It is a region immersed in the coastal border within the Middle America Trench, Cocos Plate subduction tectonic region under the North America Plate, a territory characterized by a very complex tectonic history of folding, magmatism, and metamorphism (Yamamoto, González-Moran, et al., 2013), this seated over the Xolapa complex's metamorphic basement (Perez-Gutierrez et al., 2009; Servicio Geológico Mexicano (SGM), 1998). It is bounded by the extreme coordinates 16°47'31.5533" N, 98°33'44.9830" W and 15° 59' 23.7841" N, 97°40'30.9486" W, with an extension of 8458.7 km^2 (94.58-km x 88.76 km, Figure 1).

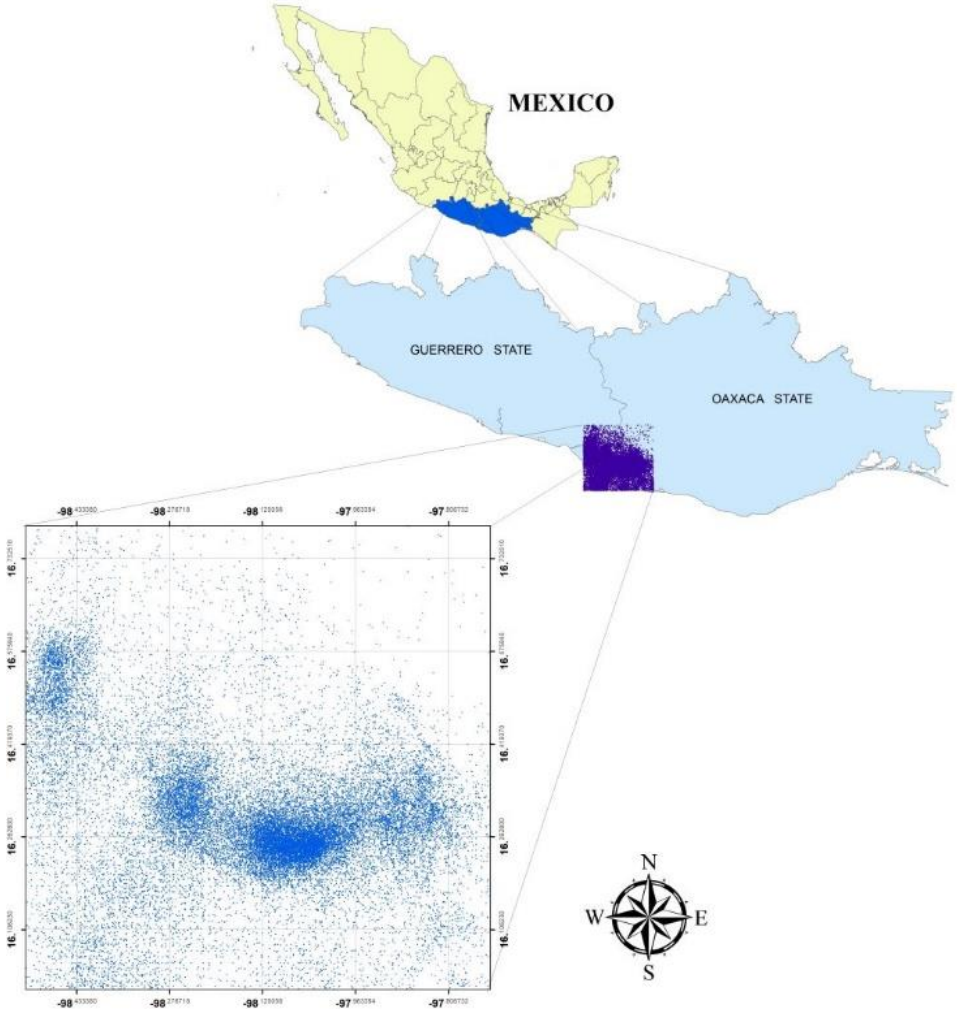

Figure 1. *Study area geographical location*

The historical antecedents of folding, magmatism, and metamorphism confer to the region under study an exceptional seismicity attributes, which has also been justified because the local continental crust could be highly fractured in several blocks that move independently

(Yamamoto, González-Moran et al., 2013). Another distinctive aspect of the study area and its surrounding area is the manifestation of pairs of significant earthquakes (<5.5Mw) or also so-called doublet, EQs with very close magnitudes (0.2Mw units) and no more than 100 km away from each other (Martínez-García, 2017; Martínez-García et al., 2015, 2016; Riga & Balocchi, 2018; Yamamoto et al., 2002; Yamamoto, González-Moran, et al., 2013). An example of this earthquake is the event that occurred on June 7, 1982 (6.9, 7.0 Mw).

2. METHOD

In this study, 32,046 seismic records (2.0 to 7.5Mw, 1980 to 2021 period) obtained from the National Seismological Service catalog (SSN, UNAM, Mexico, Doi: 10.21766/SSNMX/EC/MX) were analyzed, 21 of them are considered significant earthquakes (5.5 to 7.5Mw) and the last one occurred on February 16–19, 2018 (7.2 and 6.0Mw). After that date, 20176 seismic events occurred but none were considered significant (5.3–2.0 Mw)

The original table "txt" format with plain text containing the earthquake data list was exported to the geographic information system (*ArcGis Desktop* 10.6 and *Global Mapper* V18). This geographic tool contributed significantly to the initial analysis and allowed the display of a bunch of geographically referenced information about the study area. (Toma-Danila et al., 2017).

To identify the most statistically significantly related data value clusters, an analysis series of LISA (Local Indicators of Spatial Association) and Moran's I maps, was conducted with the purpose to obtain cluster maps through spatial autocorrelation data exam using a Spatial Data Science Tools (SDScT, *GeoDa* 1.20.0.8) (Zhang et al., 2009). Spatial autocorrelation analysis, namely the global and local spatial autocorrelation test, Moran's I index is considered a reliable strategy for identifying patterns applied in seismology, it has been used in Romania (Bucharest), Indonesia (Tripa Fault in Aceh Province), Iran, China (mainland China and Alpine Himalayan), Pakistan, which has provided consistent results locating seismic hot spots, spatial configurations of earthquake events, earthquake clusters, besides spatiotemporal dynamic, mechanisms and characteristics of seismic activity (Al-Ahmadi et al., 2014; Armaş, 2012; Aslam & Naseer, 2020; Cao et al., 2022; Catita et al., 2019; Harini, 2019; Li et al., 2020; Sofyan et al., 2019; Toma-Danila et al., 2017; Yousefzadeh et al., 2021). This approach and the applied statistical method employed in this paper are considered unprecedented in their application to the identification of patterns in the spatial distribution of seismic events in MAT.

Each SHP format table was set in *SDScT* using the Space - Univariate Local Moran's I menu option (SULMI), setting the magnitude variable. Previous has attained the spatial weights file (GAL file), a simple text file that contains the number of neighbors and their identifiers for each observation.

As a result, the LISA cluster map is obtained according to the series of earthquakes involved in each study period (1980 to 2021). SULMI has been applied to reveal that EQ spatial distribution records are not randomness but clustering. Moran's I statistic for spatial correlation is established as the following:

$$I = \frac{n}{S_0} \frac{\sum_{i=1}^{n} \sum_{j=1}^{n} w_{i,j} z_i z_j}{\sum_{i=1}^{n} z_i^2}$$

The details of the statistical principles applied in this research can be consulted in the following link: https://geodacenter.github.io/workbook/6a_local_auto/lab6a.html, (Hamylton, 2013; Zhang et al., 2009).

For each EQ LISA cluster analysis, three colored map legends were obtained: not significant, high and low values clustered maps (grey, red and blue dots, respectively), emphasizing only the array of earthquakes with the largest amount of recorded data (2012 to 2021 events). The high color intensity in each map will represent a positive global spatial autocorrelation outcome, while lighter colors signify a negative spatial autocorrelation.

3. RESULTS

Within the study area among the states of Guerrero and Oaxaca coastal limits, Mexico, from January 1,

1980, to December 31, 2021, 21 significant earthquakes (5.5 to 7.5Mw) have been felt, these and 32,025 events less intense were analyzed applying some series of LISA and Univariate Local Moran's I tool.

From 1980 to 2011, just 1730 seismic events (5.4% including 11 significant events) of the 32,046 records used for this study occurred, but the lack of data in this period was not entirely attributable to poor seismic network coverage, at least for the first nine years of the interval under study (Armendáriz, 2006). From 2012 to 2021 there was a significant increase (Figure 2, Table 1), reaching a maximum peak of 27.7% (8861 events) in 2018 (UNAM, 2013), after this year, the seismic activity progressively decreased, in 2019 (16.0%), 2020 (11.5%) and 2021 (8.79%) respectively, this distribution includes eight events considered significant (5.5 to 7.5Mw).

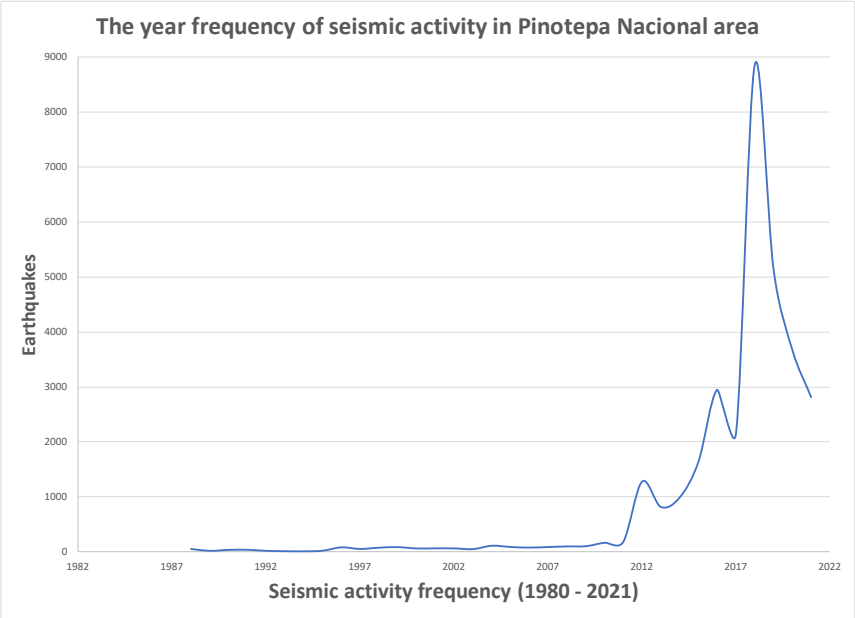

Figure 2*. 40 years of seismic activity in the Pinotepa Nacional region*

Based on the statistical reliability of the expected results, this trend led to identifying the ideal period to apply the LISA and SULMI analysis that would allow identifying the spatial patterns of the region seismicity data, this period was from 2012 to 2021 (Table 1). Ten LISA cluster maps were obtained for the years 2012-2021 (Figure 3).

Table 1. LISA cluster data analysis, period 1980 to 2021

EARTHQUAKE	1980-1987	1988	1996	1997	2002	2004	2005	2010	2012	2013	2014	2015	2016	2017	2018	2019	2020	2021
Total EQ data	25	55	84	55	65	113	91	167	1279	820	989	1639	2948	2155	8861	5136	3673	2816
Mw (significant)	6.9, 7.0, 5.9, 5.5 (4)	0	5.5	5.6	5.5	6.4	5.8	6	7.5, 6.0	0	5.5, 5.7	0	6.0, 5.7	0	7.2, 6.0	0	0	0
No significant	20	37	76	47	55	104	83	148	1085	710	844	1424	2568	1885	6914	4289	3058	2380
High	2	8	2	3	1	2	0	2	47	26	45	68	114	70	692	255	169	120
Low	2	7	5	2	3	0	2	4	83	42	50	45	114	79	645	293	229	146
Low - High	1	1	0	0	5	4	3	7	30	28	24	37	89	79	228	156	105	92
High - Low	0	2	1	3	1	3	3	6	34	14	26	65	63	42	382	143	112	78

Mw = moment magnitude scale
It is omitted years without significant seismic events (<5.5Mw)

Identified ideal period for analysis

Year	High - High	Low - Low	No significant
2012		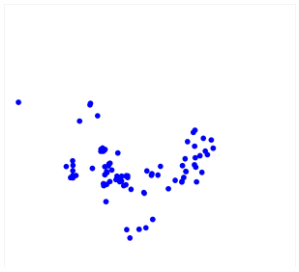	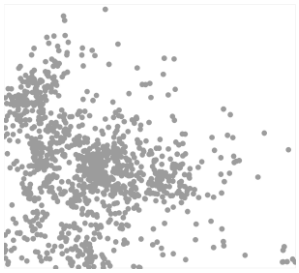
2013		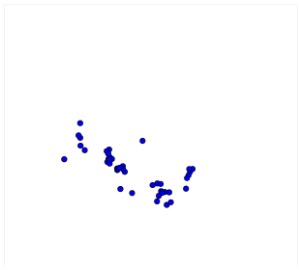	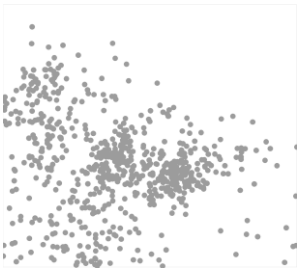
2014	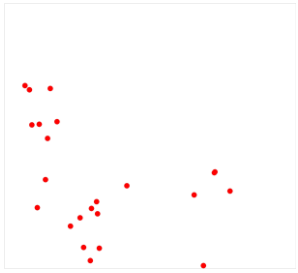	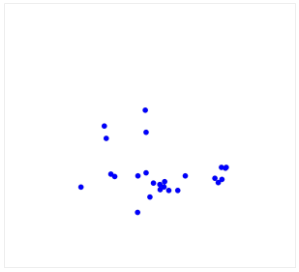	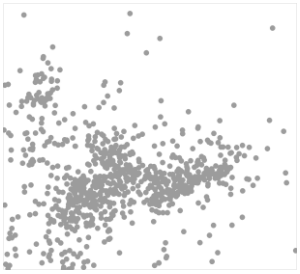
2015	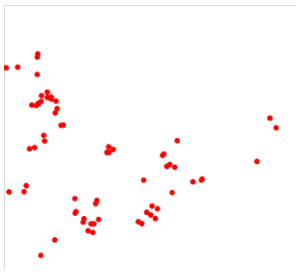	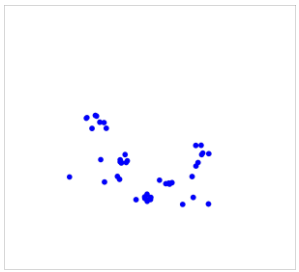	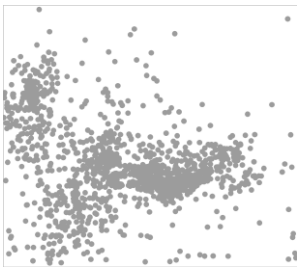
2016	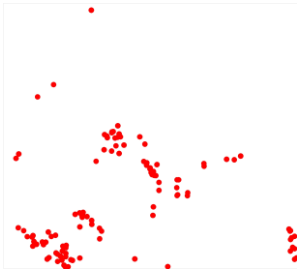	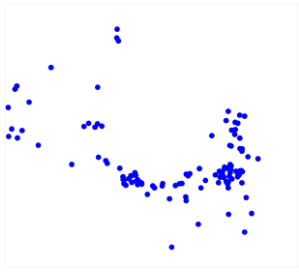	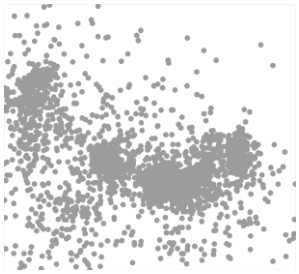
2017		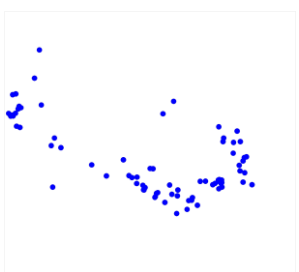	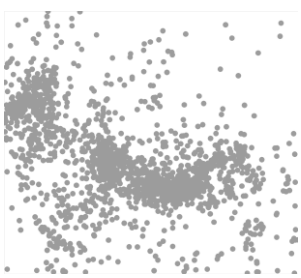

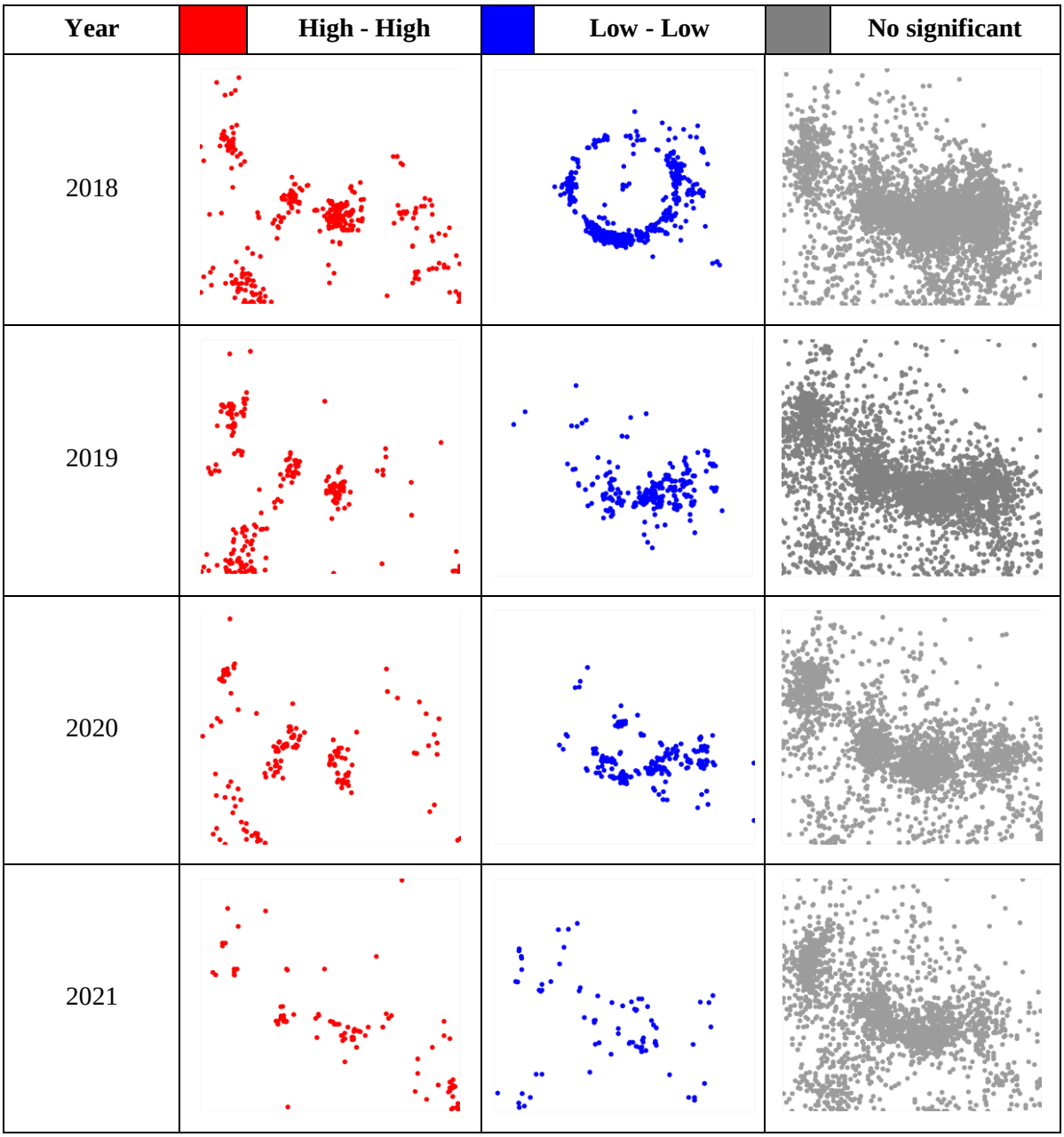

Figure 3. *Local Indicators of Spatial Association (LISA) clusters EQ maps from 2012-2021*

SULMI analysis results show a conclusive tendency to cluster in specific spatial directions. The statistical significance analysis among data shows that only on average 21% of the data are subject to cluster to peculiar areas of the geographic space under study, which suggests that they are associated with three very particular processes within the local seismic activity (Figure 3), namely,

- Potential zones of significant seismicity and foreshocks-mainshock-aftershocks events (Figure 3, *High-High column*), dots in red.
- Structures or geographical hidden tectonic features (Figure 3, *Low-Low column*), dots in blue, data particularly associated with 2018.
- Continuous subduction movement (Figure 3, *No significant column*), dots in gray.

To be more consistent in the delineation of possible hidden tectonic features observed in the map (Figure 3, 2018, blue dots), the data with the greatest significant spatial association were filtered saving in a separate SHP file (*GeoDa Tool)*, considering only the field of Magnitude (micro-seismicity) and depth, in the intervals of

2.0-2.9Mw and 10 km depth preferentially, this procedure, the delineated structure was more evident, and likewise is aligned with the 21 significant earthquakes (5.5 to 7.2 Mw) occurred in the surrounding area from 1980 to 2021 (Figure 3, *Low-Low column*; Figure 4).

The patent evidence of the structure presence referred to above is the delineation of almost circular shape shown on the LISA cluster map in Figure 3, *Low-Low column*. The tectonic nature of this structure is unknown, it is a form that was delineated only after the two earthquakes of 7.2 and 6.0 that occurred on February 16 and 19, 2018 but narrowly related to 579 earthquakes (Figure 3, *blue dots column*) with magnitudes from 2.0 to 2.8, 54.0% of 1846 statistically significant data (red and blue dots) recorded from the earthquake occurred in 2018, almost all of them located to almost 10 km depth, the shape delineated has a diameter of 43 km approximately (Figure 4).

The reliability of the results related to the structure located 10 kilometers over the surface also suggests that there is some kind of very particular spatial autocorrelation worth studying, therefore such an argument was revalidated using two statistic procedures. The first was modifying the significance value limits from P = 0.05 to P = 0.01 and increasing the number of interactions from 999 to 9999.

Another technique was to apply two statistical indicators, the first is the Geary Local Univariate statistic (Geary LU) is another Local Indicator of Spatial Association (LISA) that focuses on squared differences, or dissimilarity. It is a complementary statistic to Moran's I, giving inverse processing to the data, statistics small values suggest positive spatial autocorrelation and *vice versa*.

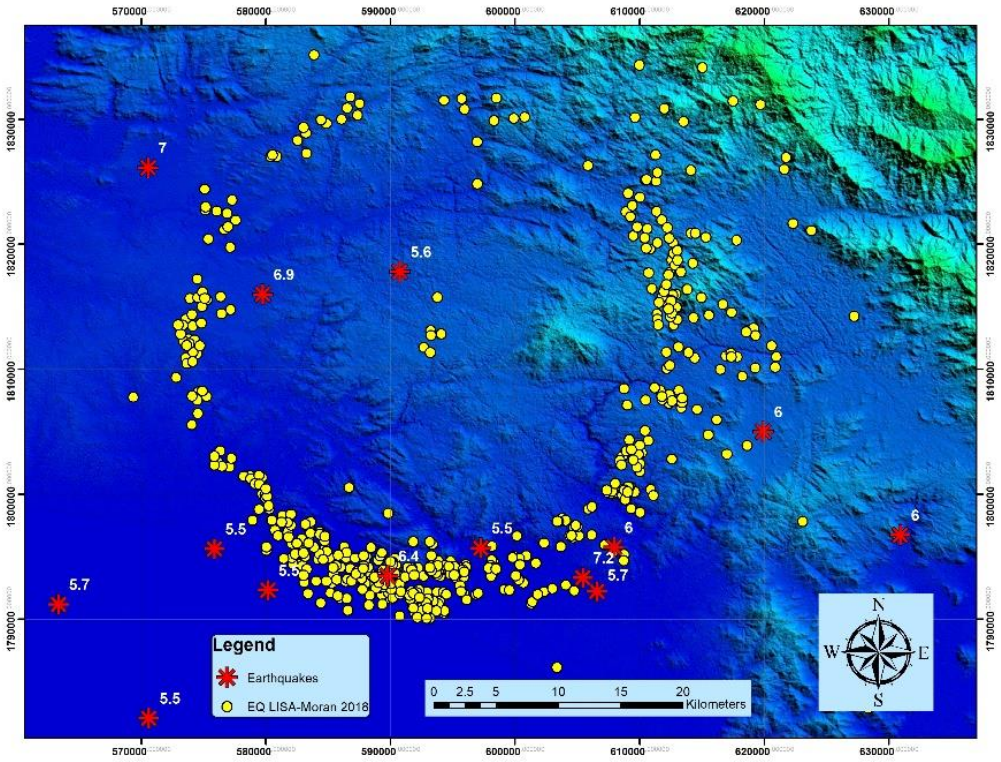

***Figure 4**. Spatial alignment between Figure 3 (Low-Low column), data (2018), and earthquakes that occurred around*

The second statistic was the Getis-Ord Local Univariate (Gi* LU) which is interpreted as the relationship of each datum, a high value must be surrounded by other features with high values, as result, high values or greater than the mean represent high-high clusters or *hot spots* and low values or less than the mean indicates Low-Low cluster or *cold spot*. The result of the revalidation process described above is included in Figures 5 and 6.

4. DISCUSSION

With the LISA and SULMI analyses have been possible to identify theoretically, the spatial patterns of the most statistically significant seismic data (21.0%). The potential clusters of seismicity data recognized allow us to affirm that there is an assembly of data whose distribution in the study area is not entirely random.

Año/Mw	9999 per, P = 0.05	9999 per, P = 0.01	9999 per, P = 0.001
2018 Mw: 2.0 to 2.8 Low values	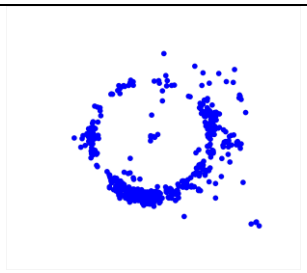	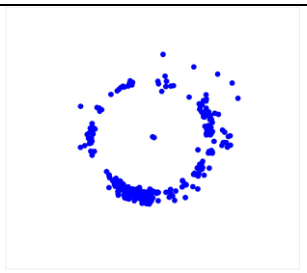	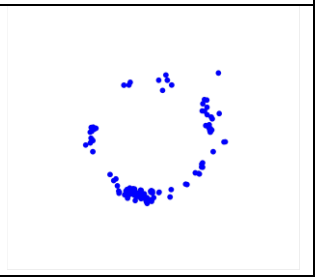
2018 Mw: 3.3 to 4.6 High values	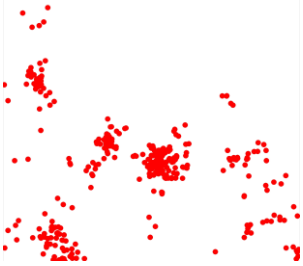	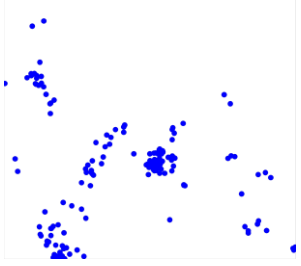	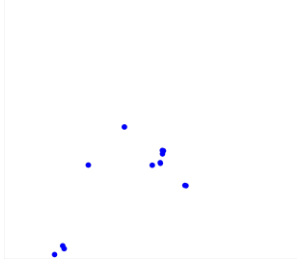

Figure 5. *Results of the modification to the permutation and P values data from the year 2018*

Año/Mw	SULMI	Gi*LU	Geary LU
2018, Low values; Moran's I; Mw: 2.0 to 2.8. GT; Mw: Mw: 2.0 to 4.7. Geary LU; Mw: 2.0 to 3.2	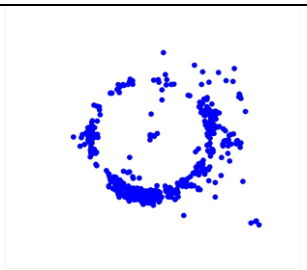	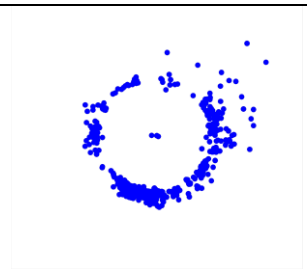	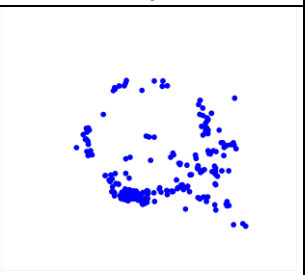
2018, High values Moran's I; Mw: 3.3 to 4.6. GT; Mw: Mw: 2.4 to 4.6. Geary LU; Mw: 3.3 to 4.6	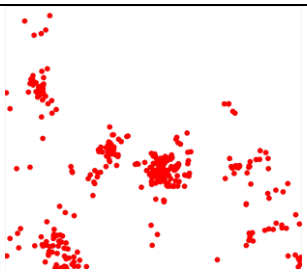	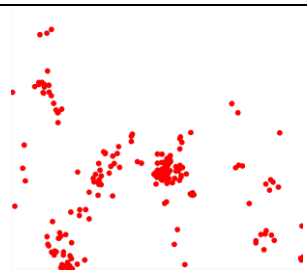	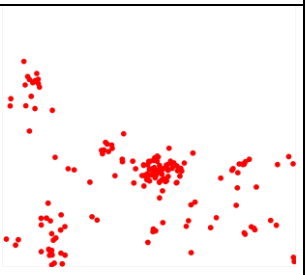

Figure 6. *Validation results of Gi*LU and Geary LU statistics applied to 2018 seismic data*

About 21.0% of information is related to potential zones of significant seismicity, foreshocks-mainshock-aftershocks events (4 to 7.5Mw), and structures or geographical hidden tectonic features (2 to 2.8Mw), data that are interspersed with a wide percentage of seismic information (2.9 to 3.9Mw) associated with the continuous subduction movement between the Cocos Plate and the MAT (79.0%).

The 2018 data suggest the presence of a tectonic structure, an almost circular shape included in the LISA cluster map of 2018 (Figure 3, *Low-Low*

column). The presence of the structure delineated within the study area could provide an alternative response to the intense local seismic activity since 14 earthquakes occurred and are closely aligned with such structures, Table 2.

Table 2. Earthquakes most significant from 1982 to 2018

No	Date	Hour	Mw	LN	LW	Depth
1	07/06/1982	00:52:33	6.9	16.424	-98.253	6
2	07/06/1982	04:59:40	7	16.516	-98.339	19
3	14/12/1982	08:11:51	5.7	16.46	-98.51	16
4	21/01/1997	15:19:58	5.6	16.44	-98.15	18
5	14/06/2004	17:54:21	6.4	16.22	-98.16	10
6	13/08/2005	21:51:58	5.8	15.99	-98.4	15
7	30/06/2010	02:22:27	6	16.24	-97.99	4
8	20/03/2012	12:02:48	7.5	16.264	-98.457	18
9	02/04/2012	12:36:43	6	16.2948	-98.544	12
10	24/05/2014	03:24:46	5.7	16.2002	-98.4073	4
11	08/05/2016	02:33:59	6	16.323	-97.8773	7
12	27/06/2016	15:50:31	5.7	16.208	-98.003	4
13	16/02/2018	17:39:39	7.2	16.218	-98.0135	16
14	19/02/2018	00:56:58	6	16.2477	-97.775	10

The presence of the delineated structure within the zone perhaps may be correlated, in the first instance, with the regional geological history of folding, magmatism, and metamorphism (Figure 7), this may be an ancient magmatic intrusion of material from the earth's mantle favored by the existence of remaining tectonic vulnerabilities. According to the outlined object dimensions, it could be associated also with an age-old volcanic arc that results in an ancient volcanic caldera, a batholith, a volcanic chamber, or a duct. However, its large dimensions and its almost circular shape could be associated with an ancient impact of an asteroid, particularly due to the existence of the mountainous relief deformation seen to the north of the structure (Figures 8–9).

The notable physical evidence of relief deformation and the slight bulge (dome) in the center of the structure are very similar to characteristics observed to those existing in other impacts recorded in other regions of the Earth's surface (Figure 8, DEM source: https://asterweb.jpl.nasa.gov/gdem.asp).

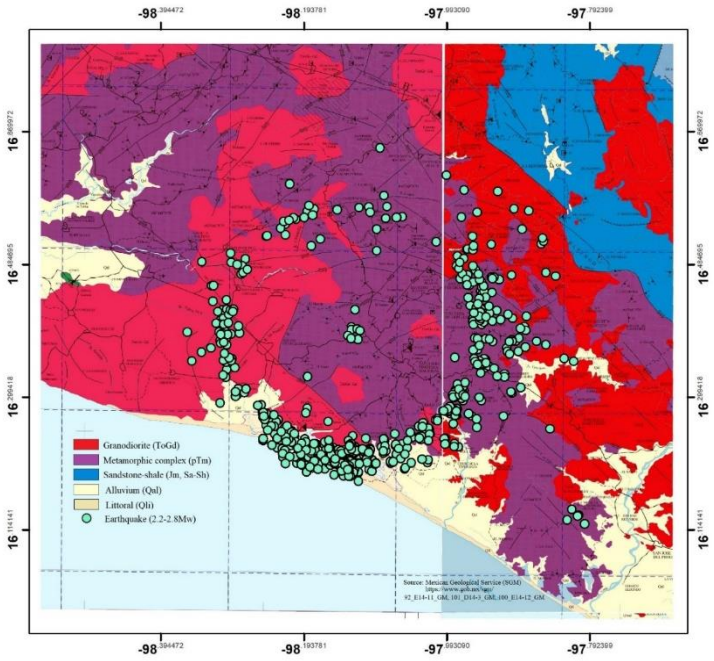

***Figure 7**. Geology characteristics around the structure delineated within the area thru 2018 seismic activity*

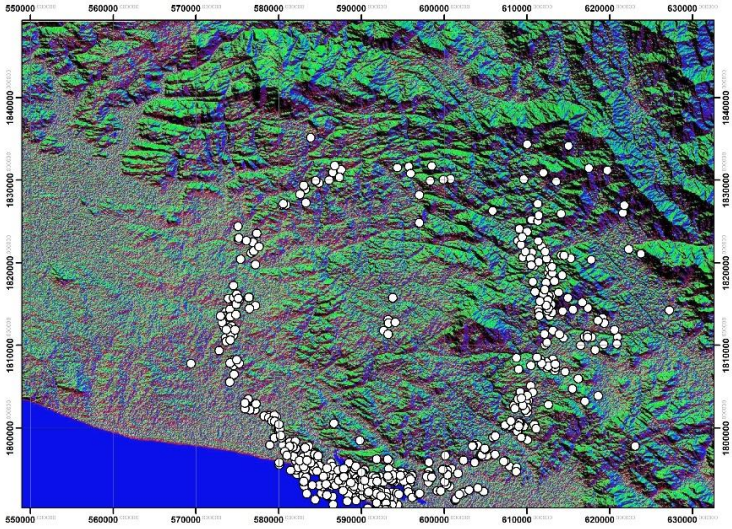

***Figure 8**. Evidence of relief deformation to North of the tectonic feature delineated*

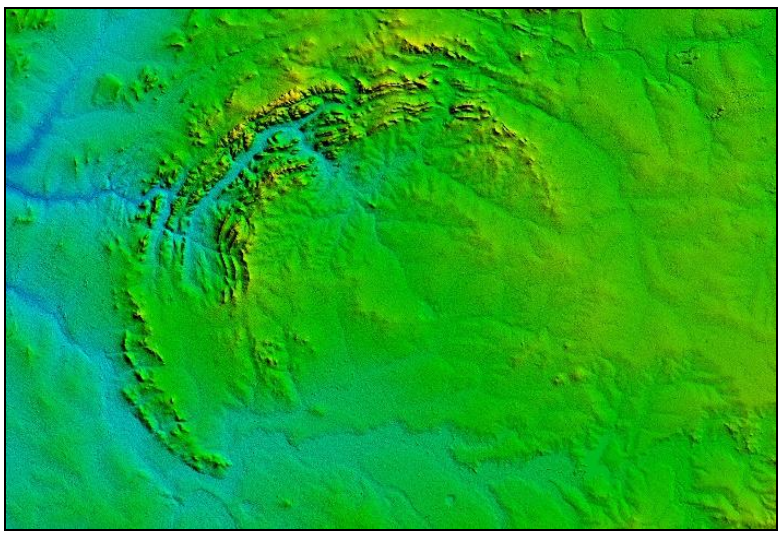

***Figure 9**. Vredefort Crater, Free State, South Africa, with almost 40 km inside diameter*

5. CONCLUSIONS

The seismic activity within the region under study from 1980 to 2021 registered 32,046 earthquakes. However during a period of 30 years (1980 to 2011), the number of seismic events represented only 5.4% of the records.

From 2012 to 2021 there was a significant increase, reaching a maximum peak of 27.7% (8861 events) in 2018 (UNAM, 2013), after this year, the seismic activity progressively decreased, in 2019 (16.0%), 2020 (11.5%) and 2021 (8.79%) respectively.

The space-time distribution of 32,046 earthquakes over 42 years is not randomly, earthquakes are associated with particular regions within the study area.

a) Continuous subduction movement (79% of data, considered "statistical noise").
b) The 21.0% remaining data suggest potential zones of significant seismicity (at least >5.5Mw) and foreshock-mainshock-aftershock events.
c) And some records suggest (2.0 to 2.8Mw) the presence of hidden structures or tectonic features within the study region.

The local seismic data pattern analyzed has contributed to delineating forms hidden beneath the area's surface as mentioned in this document, located just a few kilometers below. Micro-seismicity between 2.0 and 2.8 Mw originated principally in 2018 and showed a geographical feature hidden until now. It is a shape that is 43 kilometers in diameter, hidden 10 kilometers deep.

The results obtained with the application of the Gi*LU and Geary LU statistics to the records of 2018 suggest that the probability that the spatial arrangement (2.0 to 2.8Mw earthquakes) obtained at *P=0.05* and *0.01* of significance level responds to some type of spatial autocorrelation that is worth studying (Figure 3, *Low-Low column*; Figures 5-6*)*. This supports also the clustering results of potential zones of significant seismicity (>5.5Mw) and foreshock-mainshock-aftershock events also applicable to years before and after 2018.

The focus and results carried out with LISA and SULMI referred to seismic pattern analysis applied to Pinotepa seismic region can be considered outstanding with the potential for application to other seismic geographical regions.

The approach applied to study the seismicity data in the region evaluated, demonstrated to be a sensitive statistical tool and adequate (*Geoda tool*), with filters that make it possible to tabulate with certain precision the numerical limits between the data clusters (grey, red and blue dots), which would allow choosing only those data statistically significant to the seismic variations monitoring, spectra and waveforms study and forecasting future seismic events (spatial path, direction, and trend), even considering that each significant event has its own characteristics, as could be the case of the region under study.

REFERENCES

Al-Ahmadi, K., Al-Amri, A., & See, L. 2014, 'A spatial statistical analysis of the occurrence of earthquakes along the Red Sea floor spreading: Clusters of seismicity'. *Arabian Journal of Geosciences*, *7*(7), 2893–2904. https://doi.org/10.1007/s12517-013-0974-6

Arai, S. 1982, 'Petrology of Basalts from Site 487, Deep Sea Drilling Project Leg 66, Middle America Trench Area off Mexico'. In *Initial Reports of the Deep Sea Drilling Project, 66* (I, pp. 711–722) U.S. Government Printing Office. https://doi.org/10.2973/dsdp.proc.66.134.1982

Armaş, I. 2012, 'Multi-criteria vulnerability analysis to earthquake hazard of Bucharest, Romania'. *Natural Hazards*, *63*(2), 1129–1156. https://doi.org/10.1007/s11069-012-0209-2

Armendáriz, E. 2006, 'Estación Linares (CENAPRED-UANL) nuevo observatorio de la Red Sismológica Nacional'. *Ciencias UANL*, *IX*(002), 192–196.

Aslam, B., & Naseer, F. 2020, 'A statistical analysis of the spatial existence of earthquakes in Balochistan: clusters of seismicity'. *Environmental Earth Sciences*, *79*(1). https://doi.org/10.1007/s12665-019-8790-2

Bianco, M. J., Gerstoft, P., Olsen, K. B. & Lin, F. C. 2019, 'High-resolution seismic tomography of Long Beach, CA using machine learning'. *Scientific Reports*, *9*(1), 1–11. https://doi.org/10.1038/s41598-019-50381-z

Cao, Z., Zhang, H., Liu, Y., Liu, S., Feng, L., Yin, L., & Zheng, W. 2022, 'Spatial distribution analysis of

seismic activity based on GMI, LMI, and LISA in China'. *Open Geosciences*, *14*(1), 89–97. https://doi.org/10.1515/geo-2020-0332

Carr, B. J., Smithson, S. B., Kareav, N., Ronin, A., Garipov, V., Kristofferson, Y., Digranes, P., Smythe, D., & Gillen, C. 1996, 'Vertical seismic profile results from the Kola Superdeep Borehole, Russia'. *Tectonophysics*, *264*(1–4), 295–307. https://doi.org/10.1016/S0040-1951(96)00133-3

Catita, C., Teves-Costa, M. P., Matias, L., & Batlló, J. 2019, 'SPATIAL DISTRIBUTION OF FELT INTENSITIES FOR PORTUGAL EARTHQUAKES'. *The International Archives of the Photogrammetry, Remote Sensing and Spatial Information Sciences*, *XLII-3/W8*(3/W8), 87–92. https://doi.org/10.5194/isprs-archives-XLII-3-W8-87-2019

Dominguez, L. A., Taira, T., & Santoyo, M. A. 2016, 'Spatiotemporal variations of characteristic repeating earthquake sequences along the Middle America Trench in Mexico'. *Journal of Geophysical Research: Solid Earth*, *121*(12), 8855–8870. https://doi.org/10.1002/2016JB013242

Ducea, M. N., Valencia, V. A., Shoemaker, S., Reiners, P. W., DeCelles, P. G., Campa, M. F., Morán-Zenteno, D., & Ruiz, J. 2004, 'Rates of sediment recycling beneath the Acapulco trench: Constraints from (U-Th)/He thermochronology'. *Journal of Geophysical Research: Solid Earth*, *109*(9), 1–11. https://doi.org/10.1029/2004JB003112

Hamylton, S. 2013, 'Five practical uses of spatial autocorrelation for studies of coral reef ecology'. *Marine Ecology Progress Series*, *478*(Tobler 1970), 15–25. https://doi.org/10.3354/meps10267

Harini, S. 2019, 'The earthquake events and impacts mapping in Bali and Nusa Tenggara using a clustering method'. *IOP Publishing*, *476*, 1–6. https://doi.org/10.1088/1755-1315/456/1/012087

Julian, B. R., Miller, A. D., & Foulger, G. R. 1998, 'Non-double-couple earthquakes'. *Reviews of Geophysics*, *36*(4), 525–549. https://doi.org/10.1029/98RG00716

Li, X., Yin, L., Yao, L., Yu, W., She, X., & Wei, W. 2020, 'Seismic spatiotemporal characteristics in the Alpide Himalayan Seismic Belt'. *Earth Science Informatics*, *13*(3), 883–892. https://doi.org/10.1007/s12145-020-00468-3

Martínez-García, F. 2017, 'Statistical Analysis of Natural Water Conductivity Data Behavior in Two Wells: Seismic Coastal Border Limits of Guerrero-Oaxaca States, Mexico'. *OALib*, *04*(09), 1–37. https://doi.org/10.4236/oalib.1103900

Martínez-García, F., Colín-Cruz, A., Adame-Martínez, S., & Ramírez-García, J. J. 2015, 'Atypical Variations of Water Conductivity Prior to Tectonic Earthquakes'. *International Journal of Geosciences*, *06*(12), 1367–1385. https://doi.org/10.4236/ijg.2015.612108

Martínez-García, F., Colín-Cruz, A., Pereira-Corona, A., Adame-Martínez, S., & Ramírez-García, J. J. 2016, 'Natural Water Conductivity Behavior within the Seismic Pacific Coast of Southern Mexico'. *OALib*, *03*(07), 1–21. https://doi.org/10.4236/oalib.1102836

Montalvo Arrieta, J. C., Cavazos Tovar, P., Navarro de León, I., Alva Niño, E., & Medina Barrera, F. 2008, 'Mapping Seismic Site Classes in Monterrey Metropolitan Area, northeast Mexico'. *Boletín de La Sociedad Geológica Mexicana*, *60*(2), 147–157. https://doi.org/10.18268/bsgm2008v60n2a1

Perez-Gutierrez, R., Solari, L. a, Gomez-Tuena, A., & Martens, U. 2009, 'Mesozoic geologic evolution of the Xolapa migmatitic complex north of Acapulco, southern Mexico: implications for paleogeographic reconstructions'. *Revista Mexicana De Ciencias Geológicas*, *26*(1), 201–221.

Riga, G., & Balocchi, P. 2018, 'Double Earthquakes Classification and Seismic Precursors'. *Open Journal of Earthquake Research*, *07*(01), 1–27. https://doi.org/10.4236/ojer.2018.71001

Servicio Geológico Mexicano (SGM) 1998, *Carta Geológico Minera Chilpancingo E14-8* (p. 1) Secretaría de Economía.

Sofyan, H., Rahayu, L., & Lusiani, E. 2019, 'Spatial Autocorrelation of Earthquake Magnitudes in Tripa Fault, Aceh Province, Indonesia'. *IOP Publishing*, 1–7. https://doi.org/10.1088/1755-1315/273/1/012048

Toma-Danila, D., Cioflan, C. O., & Armas, I. 2017, *GIS in seismology : contributions to the evaluation of seismic hazard and risk II*(2), 10–16. http://www.geodinamic.ro/assets/geo-patterns/volumes/v2.2_10-16.pdf

UNAM 2013, 'Ometepec-Pinotepa Nacional, Mexico Earthquake of 20 March 2012 (Mw7.5): A preliminary report'. *Geofisica Internacional*, *52*(2), 173–196. https://doi.org/10.1016/S0016-7169(13)71471-5

Yamamoto, J., González-Moran, T., Quintanar, L., Zavaleta, A. B., Zamora, A., & Espindola, V. H. 2013, 'Seismic patterns of the Guerrero-Oaxaca, Mexico region, and its relationship to the continental margin structure'. *Geophysical Journal International*, *192*(1), 375–389. https://doi.org/10.1093/gji/ggs025

Yamamoto, J., Quintanar, L., & Jiménez, Z. 2002, 'Why earthquake doublets in the Ometepec, Guerrero, Mexico subduction area?'. *Physics of the Earth and Planetary Interiors*, *132*(1–3), 131–139. https://doi.org/10.1016/S0031-9201(02)00048-1

Yousefzadeh, M., Hosseini, S. A., & Farnaghi, M. 2021, 'Spatiotemporally explicit earthquake prediction using deep neural network'. *Soil Dynamics and Earthquake Engineering*, *144*. https://doi.org/10.1016/j.soildyn.2021.106663

Zhang, L., Ma, Z., & Guo, L. 2009, 'An evaluation of spatial autocorrelation and heterogeneity in the residuals of six regression models'. *Forest Science*, *55*(6), 533–548. https://doi.org/https://doi.org/10.1093/forestscience/55.6.533

GIS software references

Blue Marble Geographics. 2018, Global Mapper v18.0.0. Hallowell, Maine 04347 U.S.A.

Environmental Systems Research Institute (ESRI). 2017, ArcGIS Release 10.6. Redlands, CA.

GeoPatterns, Vol. VII (2022), pp. 34-44, https://doi.org/10.5719/GeoP.7/3

Flood hazard and vulnerability-related research in Romania. The Gordian knot of conceptual and operational overlapping

ANDRA-COSMINA ALBULESCU

Alexandru Ioan Cuza University of Iasi, Tulnici Research Station RECENT-AIR,
Faculty of Geography and Geology, Romania
cosmina.albulescu@uaic.ro

Abstract. Scientific research is of critical importance for salient decision-making aiming to reduce flood risk, but the interwoven character of risk-related terminology and the demanding task of operationalising concepts like hazard and vulnerability frequently hinder scientific advancement. This paper documents the i) meaning of the terms hazard and vulnerability, and ii) operationalisation of these concepts, in the scientific research focusing on river floods in Romania. A 4-step semi-systematic literature review was performed, setting the time frame to 2000-2022. The literature review points out the conceptual and operational overlapping of the flood hazard and vulnerability, as well as their dynamics and spatial focus. Flood hazard is operationalised mostly through hydraulic modelling and spatial analysis, while flood vulnerability is frequently assessed via index-based methodologies. There are several studies that operationalise flood vulnerability or hazard using a methodology that targets flood risk. Another tendency observed in the literature is to choose titles referring to one of the flood risk components, but to formulate aims that concern the other; in certain cases only to assess their intersection. By addressing these issues, we aim to open the way to flood hazard and/or vulnerability assessments that properly fit the terminological and methodological paradigms.

Keywords: flood hazard, flood vulnerability, risk terminology, Romania flood

1. INTRODUCTION

Floods represent prevalent, high-impact natural hazards that can easily lead to disasters or crisis situations, given the appropriate vulnerability conditions. Flood events were estimated to account for approximately 0.5 billion deaths, also affecting over 2.8 billion people in 1980-2009 (Doocy et al. 2013), and 2 billion people in 1998-2017 (WHO 2020). Optimistic perspectives are shown by the decrease in flood-determined fatalities in 1960-2013 (Tanoue et al. 2016), but the impact of future floods may be augmented by climate change (Mandel et al. 2021), in conjunction with increased exposure of population and assets (Rentschler et al. 2022). Another factor worth considering refers to the economic, social, and health impact of the Covid-19 pandemic, which hindered the management of the 491 flood-related disasters reported worldwide during the first two and a half years of the pandemic (Albulescu et al. 2022).

Against this background, flood-related research proves critical, as flood management and decision-making should be grounded on scientific findings. In this context, a proper understanding of the risk-related terminology is a prerequisite not only for research aligned to international standards, but also for the efficient elaboration of flood mitigation plans and flood risk reduction strategies.

Nevertheless, there are two notable challenges that arise in any research effort concerning natural risks. The first refers to the intricate and wide-range definitions of risk terminology, which stem from the integration of the risk, hazard, and vulnerability terms many scientific disciplines, each with its own definitions, ontology, and methodological approach (Hufschmidt 2011). This leads to semantic fragmentation, scientific inconsonances and transform comparisons into puzzling tasks. The second challenge consists in the conundrum of operationalising the risk, hazard and vulnerability concepts.

This paper aims to document the i) meaning of the hazard and vulnerability terms related to floods, and ii) operationalisation of these concepts, in the scientific research published in 2000-2022, focusing on river floods in Romania. The study area was selected based on its significant flood risk that results from the intersection of high-level flood hazard and vulnerability (FHV). Liu et al. (2022) place Romania on the 30th place in the world in terms of flood frequency, and the fact that more than half of the disasters registered in 1990-2016 are linked to flood events (Zaharia and Ioana-Toroimac 2017) proves that the country displays strong vulnerability conditions.

This is the first literature review that focuses on the use of risk-related terminology in Romania. It contributes to our understanding of the Romanian perspective on FHV, and may represent a source of future research ideas. In addition, it helps to identify convergence points and inconsonances between place- or scale-dependent research perspectives and the internationally accepted terminology.

2. RISK-RELATED TERMINOLOGY

The terms that are most subject to divergent definition and implicitly various operationalisation approaches are risk, hazard, and vulnerability; these are complemented by resilience, exposure, susceptibility/sensitivity, etc.

Risk is defined as "the potential loss of life, injury, or destroyed or damaged assets which could occur to a system, society or a community in a specific period of time, determined probabilistically as a function of hazard, exposure, vulnerability and capacity" (UNDRR 2022). The elements of the aforementioned function may vary (Villagran de Leon 2006), but the ones that are indispensable to any definition are hazard and vulnerability, which also support multiple interpretations.

A hazard designates a "process, phenomenon or human activity that may cause loss of life, injury or other health impacts, property damage, social and economic disruption or environmental degradation" (UNDRR 2022), but it is also viewed as the probability of occurrence of such a process or phenomenon in a certain region and time frame (Cardona 2003, Birkmann et al. 2014).

The term vulnerability presents an even wider palette of definitions, as shown by numerous literature review papers (Adger 2006, Villagran de Leon 2006, Fuchs et al. 2011, Hufschmidt, 2011). The definition evolved from the factor of internal risk to a multidimensional concept (Birkmann 2013). The first stages of evolution focus on the dimensions of potential loss and damage (supported by the elements at risk) caused by the manifestation of a hazard (Coburn et al. 1994), while the multifaceted and dynamic attributes of the concept are best portrayed by the UNDRR (2022) definition: vulnerability is the totality of "conditions determined by physical, social, economic and environmental factors or processes which increase the susceptibility of an individual, a community, assets or systems to the impacts of hazards". This definition relies on susceptibility, which represents the tendency of a certain area to be affected by a phenomenon with destructive potential (Dominguez-Cuesta 2013).

In this paper, all the terms in risk research are integrated into river floods and flash floods contexts, and the definitions provided by the United Nations Disaster Risk Reduction Glossary (UNDRR 2022) are held as standard, internationally accepted ones.

3. METHODOLOGY

The semi-systematic literature review concerning the FHV research in Romania was a 4-step process (Figure 1), coordinated by the following research questions:

- How are the FHV concepts defined/interpreted and operationalised in the autochtonous scientific literature?
- How did the FHV operationalisation evolve in time (2000-2022)?
- Are the autochtonous operationalisations concordant with the international, official definitions of risk-related terminology?

Both risk components were reviewed by introducing specific keywords (i.e., "flood hazard Romania", "flood vulnerability Romania") into academic search engines (e.g., Google Scholar, Web of Knowledge, ResearchGate). At this stage, a total of 44 papers written in English were collected, each of them including "hazard", "vulnerability", or

"susceptibility" in their title or keyword list, concurrently stating the aim of assessing the risk components mentioned above in a "flood" and/or "flash-flood" context.

The exclusion criteria referred to the relevance of the research topics for the operationalisation of the FHV. For instance, scientific papers concerning soft and hard flood hazard mitigation methods, as well as particular flood hazard events were excluded from the literature review, due to the fact that they do not add to the operationalisation of the FHV. Papers referring to dam failure and associated flood modelling were also left out of the review, because they focus on flood risk and not particularly on one of its components. Subsequently, assessments that consider other destructive processes and phenomena in addition to floods, were excluded from the list, since the review concerns specifically flood hazard or vulnerability. Finally, the papers that did not meet basic academic standards (i.e., organised structured, well-explained methodological framework, reproducible results) were deleted from the list of considered research works. To gain as broad a perspective as possible, the type of paper (e.g., literature review, research article, technical note/report) or the journal metrics were not included on the list of exclusion criteria.

The resulting batch of 28 articles was thoroughly read and analysed, comparing their findings with the official definitions of hazard and vulnerability. In addition, a database of indicators integrated in flood vulnerability assessments was constructed (Appendix 1).

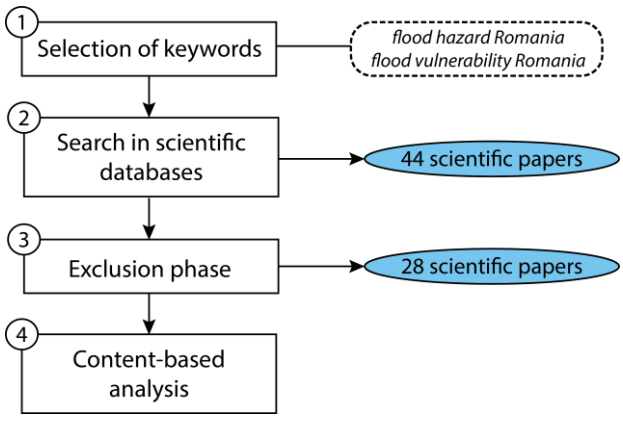

Figure 1. *Methodological workflow of the literature review*

4. RESULTS

Research on flood hazard

The number of selected articles concerning flood and/or flash flood hazard is rather low (8), due to the fact that only the ones that specifically use the term hazard in their title, aim or keyword list were included. The papers with titles that exclude the term of interest, but comprise "flood/flash flood potential" were considered to refer to flood risk, and not specifically to the flood hazard. Half of the research papers were published since 2019, and only two of them were written during the Covid-19 pandemic (Figure 2). The scale of flood hazard analysis varies from national level (Mătreaţă et al. 2016) to catchment level (e.g., the lower course of the Siret, the watersheds of the Buzău, Trotuș, Niraj, Bâsca Chiojdului rivers). There are also studies that mapped flood hazard at landform unit scale (Hutanu et al. 2020) or in urban and peri-urban areas (Mihu-Pintilie et al. 2019).

The narrow batch of papers and the fact that the earliest paper of this type dates back to 2014 indicate that the hazard concept is still in its emergent stage in the Romanian scientific literature concerning floods. This evolution phase is characterised by confusion and misinterpretation of the term (Figure 2), which are highlighted by the fact that certain titles include "hazard", but the aim of the paper refers to flood vulnerability assessment (Roșca et al. 2014, Mihu-Pintilie et al. 2019, Popa et al. 2019, Hutanu et al. 2020). Also, none of the analysed manuscripts include definitions of the flood hazard.

Generally, flood and/or flash-flood hazard is analysed in terms of probability of occurrence (Roșca et al. 2014), flood extent, water depth, water elevation profiles for 10 to 100-year flood events (Țîncu et al. 2018, Mihu-Pintilie et al. 2019, Arseni et al. 2020), or runoff thresholds (Mătreaţă et al. 2016). Correct operationalisation approaches of flood hazard rely on hydraulic modelling and analysis via software designed to perform one or two-dimensional hydraulic calculations (e.g., HEC-RAS) (Mihu-Pintilie et al. 2019, Arseni et al. 2020, Hutanu et al. 2020), but there are also approaches that use the runoff coefficient (Mătreaţă et al. 2016),

or statistical and spatial analysis models (Roșca et al. 2014, Țîncu et al. 2018). However, only few of these studies include validation procedures (Costache and Zaharia 2017, Hutanu et al. 2020); which constitutes a methodological weakness.

In some cases, flood hazard is analysed together with flood risk (Roșca et al. 2014, Țîncu et al. 2018, Arseni et al. 2020), but there are also studies where hazard is operationalised as risk (Mihu-Pintilie et al. 2019, Popa et al. 2019). This deviation from proper assessment procedures is determined by the introduction of exposure-related elements in the assessments (Mihu-Pintilie et al. 2019), or by integrating both hazard and vulnerability indicators into the Flood and Flash-Flood Potential Index (Popa et al. 2019). On the other hand, Costache and Zaharia (2017) use only site-related vulnerability indicators (which make up the Flash-Flood Potential Index) to assess flood hazard, which means that the operationalisation of the hazard actually targets vulnerability (Figure 2). Another deviation from the norm constitutes the validation of the runoff coefficient-based hazard assessment using the Flash-Flood Potential Index, which integrates vulnerability-related indicators (Mătreaţă et al. 2016).

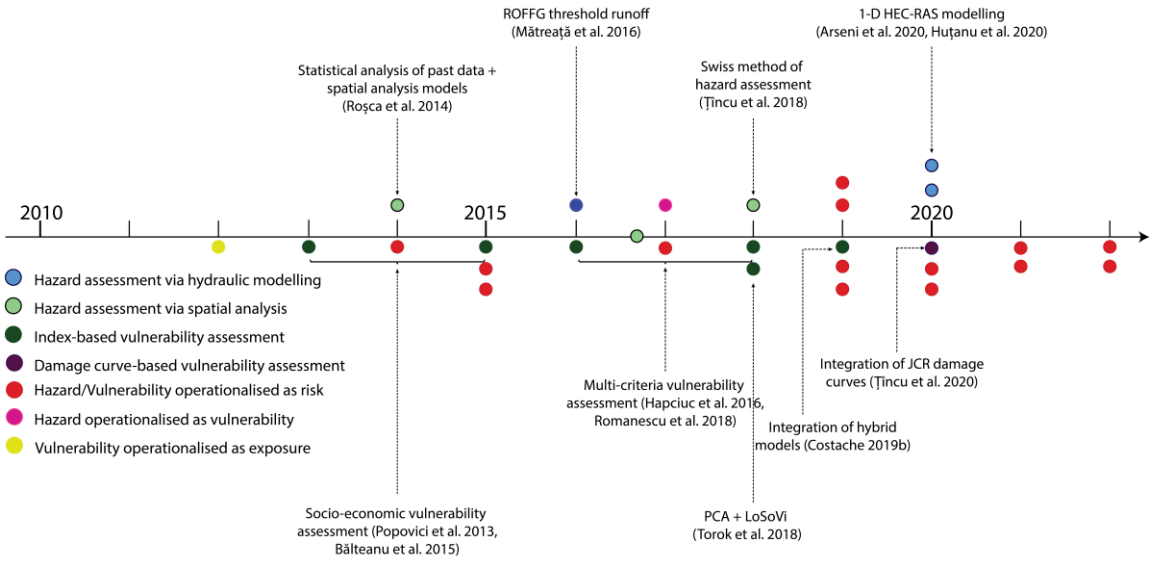

Figure 2. *Timeline of the operationalisation variants of flood hazard and vulnerability*

Research on flood vulnerability

Research concerning vulnerability to floods and/or flash floods also emerged relatively recently, the first article on the chronologically-ordered list of analysed research works dating back to 2012. Half of the 20 papers were written in 2019-2022, and 6 of them correspond to the pandemic period (Figure 2). The selection of the study areas seem to be motivated by the interest and affinity of the authors, and also by the incidence of flood events. Few studies focus on landform units (Popovici et al. 2013, Bălteanu et al. 2015, Iosub et al. 2020), and even fewer choose the national scale for the assessment of of flood vulnerability (Török 2018); meaning that catchment scale was preferred. The watersheds of the Prahova (Costache 2019a), Moldova (Popa et al. 2020), Jijia (Iosub et al. 2020), Sucevița (Hapciuc et al. 2016, Romanescu et al. 2018), Putna (Costache and Bui, 2019), Trotuș (Țîncu et al. 2020) rivers are just several of the study areas subject to flood vulnerability assessment.

The multidimensionality of vulnerability leads to a variety of ways to define and operationalise this concept. The UNDRR (2022) definition highlights the susceptibility of human communities to be affected by hazards, but it does not mention exposure, which is viewed as part of vulnerability by some scientists (Willroth et al. 2011, Birkmann 2013). Also, the coping capacity of the human communities, together with other closely related

concepts (i.e., adaptation, adjustment) are left out of the official definition, although these may alter the vulnerability level (Smit and Wandel 2006). In this literature review, all the aforementioned interpretation options were identified and analysed in direct relation to the operationalisation approaches. It has to be highlighted that in some cases, vulnerability was interpreted only using its susceptibility component, which motivates the inclusion of papers that refer to flood susceptibility in the literature review.

As vulnerability cannot be directly measured, its operationalisation in flood and/or flash flood hazard contexts, relies on indices that are aggregated in weighted or non-weighted indexes (Figure 2). The most common indicators correspond to site-related vulnerability of geological, morphological, hydrological, or pedological nature, but the pool of analysed articles also included indicators of building, socio-economic, and environmental vulnerability (Appendix 1). It should be highlighted that the values of these indicators may increase or decrease the vulnerability level, therefore partially matching the UNDRR (2022) definition which focuses on the factors or processes that increase susceptibility to harm. For example, the distance from a river may be long enough to ensure the safety of a particular building during a flood event, or too short and associated with an increased vulnerability level.

In some cases, the index-based methodologies are complemented by multi-criteria analysis (Hapciuc et al. 2016, Romanescu et al. 2018, Popa et al. 2020), and all the studies use GIS for spatial modelling and visualisation. The use of software designed to perform hydraulic calculations (e.g., HEC-RAS) is limited in flood vulnerability assessments (Romanescu et al., 2018). Another approach is to assess vulnerability based on damage curves that integrate water depth thresholds (Țîncu et al. 2020).

Like in the case of flood hazard-related studies, a prominent methodological issue concerns the validation of the results, which is often omitted (Cheveresan 2012, Popovici et al. 2013, Prăvălie and Costache 2014, Bălteanu et al. 2015, Costache et al. 2015, Zaharia et al. 2015, Hapciuc et al. 2016, Török 2018, Iosub et al. 2020, Popescu and Bărbulescu 2022).

The Romanian scientific literature on floods and flash flood vulnerability includes many examples where the purpose of assessing vulnerability is associated with a methodological framework that targets a different concept. This overlap takes the following forms:

- Vulnerability (often referred to as susceptibility) is assessed using a methodology that targets flood risk (Prăvălie and Costache 2014, Zaharia et al. 2015, Costache 2017, 2019, Costache et al. 2015, 2019a, 2021, Costache and Bui 2019, Iosub et al. 2020, Popa et al. 2020, Stoica-Fuchs 2021, Kocsis et al. 2022, Popescu and Bărbulescu, 2022). For instance, the Flood Potential Index (FPI), althogh it is defined as the occurrence potential of floods by Costache et al. (2015) – which matches the flood hazard definition of Cardona (2003), includes both susceptibility indicators and hazard indicators, making it a flood risk index. The same conceptual overlap between flood hazard and susceptibility, and risk-related operationalisation is illustrated by the Flood Susceptibility Index (Prăvălie and Costache 2014). The integration of both vulnerability/ susceptibility and hazard indicators, in the endeavour to assess the former, is also specific to the Flash Flood Susceptibility Index (Popescu and Bărbulescu 2022), the Flash Flood Potential Index (Zaharia et al. 2015, Costache 2017, Popa et al. 2020, Kocsis et al. 2022), and the Flood Potential Index (Zaharia et al. 2015, Costache 2019a), or to the approaches that combine machine learning or deep learning models (Costache et al. 2021). In many cases, these indexes integrate the amount or the intensity of rainfall, which relates to one of the factors that contribute to flood hazard, and not to vulnerability. This is because large amounts of rainfall do not make certain spaces or human communities more vulnerable to floods, but increase the probability of flood occurrence.

In addition, there are articles that aim to identify elements exposed to flash flood risk and use methodological frameworks consistent with this purpose, but that have titles relating to the

assessment of flash flood susceptibility potential (Iosub et al. 2020).

- Vulnerability is interpreted only as exposure (Cheveresan 2012), as its operationalisation is performed only through exposure indicators and does not include factors or processes that increase flood susceptibility.

A particular situation encountered in the autochthonous literature on flood vulnerability consists of correct operationalisation in the context of an erroneous definition of the concept. Costache (2019b) uses the Flash-Flood Potential Index, which integrates site-related vulnerability indicators, but refers to these as flash-flood conditioning factors, therefore attributing them to the hazard. It should be noted that the name of the index relates to flood risk, and that its selection for the purpose of vulnerability assessment deviates from the norm.

Nonetheless, there are multiple papers that define vulnerability in a proper manner (Popovici et al. 2013, Bălteanu et al. 2015, Romanescu et al. 2018), or that use the term correctly even without defining it, at the same time operationalising it adequately (Hapciuc et al. 2016, Török 2018).

5. CONCLUSIONS

The literature review points out the conceptual and operational overlap of FHV, as well as their dynamics over the last two decades (2000-2022), and the spatial focus of flood risk-related studies.

The limitations of this paper concern the exclusion of relevant research works of greater extent (e.g., doctoral theses), and of older papers that may not be available online. However, the literature review stands out as the first of its type, and allows for a deeper understanding of the ways FHV are interpreted and operationalised in the autochthonous scientific literature. Moreover, it can be a source of inspiration for future research works concerning the topic of interest.

Returning to the research questions of this study, it appears that the Romanian scientific literature includes both correct and incorrect interpretations and operationalisation approaches of the FHV concepts. The fitness of the conceptualisation and operationalisation steps within the internationally accepted research framework concerning FHV is not time dependent, as the correct interpretations and methodological frameworks alternate with those that deviate from the paradigm (Figure 2).

There are studies that operationalise flood hazard as risk, while others confuse hazard with vulnerability. In return, some flood vulnerability assessments are performed using both hazard and vulnerability indicators, meaning that they actually target flood risk. A distinctive tendency is to avoid the use of hazard or vulnerability terms, in favour of confusing terminology like “flood potential” or “flood susceptibility potential”. Also, the use of Flood or Flash-Flood Potential Index seems to be a common methodological issue of many studies that aim to analyse one of the components of flood risk, but end up constructing this index based a range of indicators that do not fit the stated research purpose. All of these examples suggest a shallow understanding of the FHV concepts.

Considering the interwoven character of risk-related terminology and its associated sense-related traps, the deviant interpretations and operationalisation approaches lead to an even more convoluted maze of risk-related research. In this context, the comparison of autochthonous findings with ones obtained in other regions of Europe or the world, becomes a fruitless effort. By bringing to light these issues, we aim to encourage flood hazard and/or vulnerability analyses that suit the terminological and methodological paradigms.

ACKNOWLEDGEMENT

Acknowledgement is given to the Operational Program Competitiveness 2014-2020, Axis 1, under POC / 448 / 1 / 1 Research infrastructure projects for public R&D institutions / Sections F 2018, through the Research Center with Integrated Techniques for Atmospheric Aerosol Investigation in Romania (RECENT AIR) project, under grant agreement MySMIS no. 127324.

A P P E N D I X 1

Table 1. Flood vulnerability indicators selected from the autochthonous scientific literature

Type of vulnerability	**Indicator**	**Reference(s)**
Site-related vulnerability	Elevation	Prăvălie and Costache (2014), Costache et al. (2015), Costache (2017, 2019a, b), Costache and Bui (2019), Costache et al. (2021), Kocsis et al. (2022)
	Slope	Prăvălie and Costache (2014), Costache et al. (2015), Zaharia et al. (2015), Hapciuc et al. (2016), Costache (2019a, b), Costache and Bui (2019), Popa et al. (2020), Costache et al. (2021), Kocsis et al. (2022), Popescu and Bărbulescu (2022)
	Length-Slope (L-S)	Zaharia et al. (2015), Costache (2017), Popa et al. (2020), Kocsis et al. (2022), Popescu and Bărbulescu (2022)
	Aspect	Costache (2017, 2019b), Costache and Bui (2019), Popa et al. (2020), Costache et al. (2021), Kocsis et al. (2022)
	Curvature/Plan curvature	Costache (2019a, b), Costache and Bui (2019), Costache et al. (2021), Popescu and Bărbulescu (2022)
	Profile curvature	Zaharia et al. (2015), Hapciuc et al. (2016), Costache (2017, 2019a), Costache and Bui (2019), Kocsis et al. (2022)
	Depth of fragmentation	Kocsis et al. (2022)
	Lithology	Prăvălie and Costache (2014), Costache et al. (2015), Zaharia et al. (2015), Hapciuc et al. (2016), Costache (2019a, b), Costache and Bui (2019), Costache et al. (2021), Kocsis et al. (2022), Popescu and Bărbulescu (2022)
	Hydrological soil groups	Costache (2019a, b), Costache and Bui (2019), Iosub et al. (2019), Popa et al. (2020), Costache et al. (2021), Kocsis et al. (2022)
	Soil type	Kocsis et al. (2022)
	Soil texture	Prăvălie and Costache (2014), Zaharia et al. (2015), Hapciuc et al. (2016), Popescu and Bărbulescu (2022)
	Soil erodibility by water	Popa et al. (2020)
	Topographic Wetness Index	Costache (2019a, b), Costache and Bui (2019), Costache et al. (2021), Kocsis et al. (2022)
	Topographic Position Index	Costache (2019b), Costache and Bui (2019), Costache et al. (2021), Kocsis et al. (2022)
	Land use/land cover	Prăvălie and Costache (2014), Zaharia et al. (2015), Hapciuc et al. (2016), Costache (2019a, b), Costache and Bui (2019), Popa et al. (2020), Costache et al. (2021), Kocsis et al. (2022), Popescu and Bărbulescu (2022)
	Distance from the river	Romanescu et al. (2018), Costache (2019a), Costache and Bui (2019), Costache et al. (2021)
	Drainage density	Costache et al. (2015), Zaharia et al. (2015), Popa et al. (2020)
	Presence of hydroengineering works	Romanescu et al. (2018)
Building vulnerability	Material of construction (buildings)	Popovici et al. (2013), Romanescu et al. (2018), Török et al. (2018)
	Building condition	Romanescu et al. (2018)
	Use of building	Romanescu et al. (2018)
Socio-economic vulnerability	Total no. of inhabitants in the affected area	Cheveresan (2012)
	Population density	Török et al. (2018)
	Average no. of people/household	Török et al. (2018)
	Density of housing units	Török et al. (2018)
	Percentage/total number of children	Cheveresan (2012), Popovici et al. (2013), Bălteanu et al. (2015), Török et al. (2018)

Type of vulnerability	Indicator	Reference(s)
	Percentage/total population of elderly	Cheveresan (2012), Popovici et al. (2013), Bălteanu et al. (2015), Török et al. (2018)
	Demographic dependency ratio	Török et al. (2018)
	No. of births/1000 inhabitants	Török et al. (2018)
	Net international migration rate	Török et al. (2018)
	Percentage of women	Török et al. (2018)
	Percentage of widow women	Török et al. (2018)
	Percentage of roma population	Popovici et al. (2013), Bălteanu et al. (2015), Török et al. (2018)
	Percentage of Hungarian ethnics	Popovici et al. (2013)
	Illiteracy rate	Török et al. (2018)
	No. of students/teacher	Popovici et al. (2013)
	Percentage of gymnasium graduates	Bălteanu et al. (2015)
	Percentage of university graduates	Popovici et al. (2013), Török et al. (2018)
	No. of doctors/1000 inhabitants	Bălteanu et al. (2015)
	No. of hospital beds per capita	Popovici et al. (2013)
	Percentage of disabled people	Popovici et al. (2013)
	Average household income	Popovici et al. (2013)
	Per capita income	Török et al. (2018)
	Employment rate	Török et al. (2018)
	Percentage of unemployment	Popovici et al. (2013), Bălteanu et al. (2015)
	Tax collection rate at local budget	Török et al. (2018)
	Percentage of people dependent on social benefits	Popovici et al. (2013)
	Entrepreneurial activity rate	Török et al. (2018)
	Percentage of service employees	Török et al. (2018)
	Percentage of agriculture employees	Bălteanu et al. (2015)
	Percentage of income from agriculture	Popovici et al. (2013)
	Herfindahl-Hirschman Index	Bălteanu et al. (2015)
	Amount of drinking water supplied to consumers	Bălteanu et al. (2015)
	Percentage of household with access to the public water supply	Popovici et al. (2013)
	Share of households with different facilities (access to piped water, sewage network, heating system, kitchen area, fixed bath)	Török et al. (2018)
	Total number of affected houses	Cheveresan (2012)
	Total number of affected roads, railways	Cheveresan (2012)
	Road density	Popovici et al. (2013), Bălteanu et al. (2015)
	Access to major public roads, railways	Török et al. (2018)
	Total number of affected domestic animals	Cheveresan (2012)
	No. of cultural heritage sites	
Environmental vulnerability	No. of protected areas	Popovici et al. (2013)
	Surface of protected areas	Cheveresan (2012)
	Ha of areas exposed to contamination because of na-tech hazards	Popovici et al. (2013)
	Total no. of landfill deposits in the affected area	Cheveresan (2012)

REFERENCES

Adger W. N. (2006) Vulnerability. Global Environment Change, 16: 268-281. https://doi.org/10.1016/j.gloenvcha.2006.02.006

Albulescu A. C., Grozavu A., Larion D. (2022) Transformări ale conceptului de multi-hazard și ale managementului său sub impactul pandemiei Covid-19 [In Romanian]. Turbulențe, discontinuități și adaptări teritoriale în Antropocen, Ed. Universtității "Alexandru Ioan Cuza" din Iași, 43-62.

Arseni M., Rosu A., Calmuc M., Calmuc,V. A., Iticescu C., Georgescu L. P. (2020) Development of flood risk and hazard maps for the lower course of the Siret River, Romania. Sustainability, 12(16). https://doi.org/10.3390/su12166588

Bălteanu D., Micu D., Costache A., Dogaru D., Persu M. (2015) Socio-economic vulnerability to floods and flash-floods in the Bend Subcarpathians, Romania, Proceedings of International Multidisciplinary Scientific GeoConference Surveying Geology and Mining Ecology Management, 577-584.

Birkmann J. (2013) Measuring vulnerability to natural hazards: towards disaster resilient societies, Second edition, Tokyo, New York, Paris: United Nations University Press.

Birkmann J., Cardona O. D., Carreño M. L., Barbat A. H., Pelling M., Schneiderbauer S., Kienberger, S., Keiler M., Alexander D. E., Zeil P., T. Welle T. (2014) Theoretical and conceptual framework for the assessment of vulnerability to natural hazards and climate change in Europe: the MOVE framework. In: Birkmann, J., Kienberger, S., Alexander, D. E. (Eds.) Assessment of vulnerability to natural hazards. Elsevier, 1-19 https://doi.org/10.1016/B978-0-12-410528-7.00001-1

Cheveresan M. (2012) Flood modeling and vulnerability assessment in Ialomita River Basin, Romania. Ohrid, Republic of Macedonia, 28: 1-11.

Coburn A. W., Spence R. J. S., Pomonis A. (1994). Vulnerability and risk assessment. Second edition, United Nations Development Programme. Disaster Management Training Programme, Cambridge: Cambridge Architectural Research Limited

Costache R. (2017) Assessment of building infrastructure vulnerability to flash-floods in Pănătău River Basin, Romania. Analele Universitățuu Din Oradea, 1: 26–36.

Costache R. (2019a) Flash-Flood Potential assessment in the upper and middle sector of Prahova river catchment (Romania). A comparative approach between four hybrid models. Science of the Total Environment, 659: 1115–1134. https://doi.org/10.1016/ j.scitotenv.2018.12.397

Costache R. (2019b) Flood Susceptibility Assessment by Using Bivariate Statistics and Machine Learning Models - A Useful Tool for Flood Risk Management. Water Resources Management, 33(9): 3239–3256. https://doi.org/10.1007/s11269-019-02301-z

Costache R., Arabameri A., Elkhrachy I., Ghorbanzadeh O., Pham Q. B. (2021) Detection of areas prone to flood risk using state-of-the-art machine learning models. Geomatics, Natural Hazards and Risk, 12(1): 1488–1507. https://doi.org/10.1080/19475705.2021.1920480

Costache R., Bui D. T. (2019) Spatial prediction of flood potential using new ensembles of bivariate statistics and artificial intelligence: A case study at the Putna river catchment of Romania. Science of The Total Environment, 691: 1098-1118. https://doi.org/10.1016/j.scitotenv.2019.07.197

Costache R., Prăvălie R., Mitof I., Popescu C. (2015) FLOOD VULNERABILITY ASSESSMENT IN THE LOW SECTOR OF SĂRĂȚEL CATCHMENT. CASE STUDY: JOSENI VILLAGE. In Article in Carpathian Journal of Earth and Environmental Sciences, 10(1) https://www.researchgate.net/publication/279316523

Costache R., Zaharia L. (2017) Flash-flood potential assessment and mapping by integrating the weights-of-evidence and frequency ratio statistical methods in GIS environment – Case study: Bâsca chiojdului river catchment (Romania). Journal of Earth System Science, 126(4). https://doi.org/10.1007/s12040-017-0828-9

Dominguez-Cuesta M. J. (2013) Susceptibility. In: Bobrowsky, P. T. (ed.). Encyclopedia of Natural Hazards. Encyclopedia of Earth Sciences Series. Dordrecht: Springer, 988-988.

Doocy S., Daniels A., Murray S., Kirsch T. D. (2013). The human impact of floods: a historical review of events 1980-2009 and systematic literature review. PLoS currents, 5. 10.1371/currents.dis.f4deb457904936b07c09daa98ee8171a

Fuchs S., Kuhlicke C., Meyer V. (2011) Editorial for the special issue: vulnerability to natural hazards – the challange of integration, Natural Hazards, 58: 609-619. DOI: https://doi.org/10.1007/s11069-011-9825-5

Hapciuc O.-E., Romanescu G., Minea I., Iosub M., Enea A., Sandu I. (2016) Flood susceptibility analysis of the cultural heritage in the Sucevita catchment (Romania). International journal of conservation science, 7(2): 501-510

Hufschmidt G. (2011) A comparative analysis of several vulnerability concepts. Natural hazards, 58(2): 621-643. https://doi.org/10.1007/s11069-011-9823-7

Hutanu E., Mihu-Pintilie A., Urzica A., Paveluc L. E., Stoleriu C. C., Grozavu A. (2020) Using 1D HEC-RAS modeling and LiDAR data to improve flood hazard maps accuracy: A case study from Jijia Floodplain (NE Romania). Water (Switzerland), 12(6). https://doi.org/10.3390/w12061624

Iosub M., Minea I., Chelariu O. E., Ursu A. (2020) Assessment of flash flood susceptibility potential in Moldavian Plain (Romania). Journal of Flood Risk Management, 13(4). https://doi.org/10.1111/jfr3.12588

Kocsis I., Bilașco Ștefan, Irimuș I. A., Dohotar V., Rusu R., Roșca S. (2022) Flash Flood Vulnerability Mapping Based on FFPI Using GIS Spatial Analysis Case Study: Valea Rea Catchment Area, Romania. Sensors, 22(9). https://doi.org/10.3390/s22093573

Liu T., Shi P., Fang J. (2022) Spatiotemporal variation in global floods with different affected areas and the contribution of influencing factors to flood-induced mortality (1985–2019). Natural Hazards, 111(3): 2601-2625. https://doi.org/10.1007/s11069-021-05150-5

Mandel A., Tiggeloven T., Lincke D., Koks E., Ward P., Hinkel J. (2021). Risks on global financial stability induced by climate change: the case of flood risks. Climatic Change, 166(1): 1-24. http://dx.doi.org/10.2139/ssrn.3626936

Mătreaţă M., Mătreaţă S., Costache R.-D., Mihalcea A., Manolache A. V. (2016) Assessment of Flash Flood Hazard Maps Using Different Threshold Values and Indices Methods. Forum Geografic, XV(Suppl. 2): 49–54. https://doi.org/10.5775/fg.2016.059.s

Mihu-Pintilie A., Cîmpianu C. I., Stoleriu C. C., Pérez M. N., Paveluc L. E. (2019) Using high-density LiDAR data and 2D streamflow hydraulic modeling to improve urban flood hazard maps: A HEC-RAS multi-scenario approach. Water (Switzerland), 11(9). https://doi.org/10.3390/w11091832

Popa M. C., Peptenatu D., Draghici C. C., & Diaconu D. C. (2019) Flood hazard mapping using the flood and Flash-Flood Potential Index in the Buzau River catchment, Romania. Water (Switzerland), 11(10). https://doi.org/10.3390/w11102116

Popa M. C., Simion A. G., Peptenatu D., Dima C., Draghici C. C., Florescu M. S., Dobrea C. R., Diaconu D. C. (2020) Spatial assessment of flash-flood vulnerability in the Moldova river catchment (N Romania) using the FFPI. Journal of Flood Risk Management, 13(4). https://doi.org/10.1111/jfr3.12624

Popescu C., Bărbulescu A. (2022) on the flash flood susceptibility and accessibility in the vărbilău catchment (romania). Romanian Journal of Physics, 67.

Popovici E.-A., Costache A., Dan B., Dogaru D., Mihaela S. (2013) Vulnerability assessment of rural communities to floods in the Western part of Romania (Banat Plain). Proceedings of International Multidisciplinary Scientific GeoConference: SGEM, 1: 1161

Prăvălie R., Costache R. (2014) Assessment of socioeconomic vulnerability to floods in the Bâsca Chiojdului catchment area. Romanian Review Of Regional Studies, 10(2).

Rentschler J., Salhab M., Jafino B. A. (2022). Flood exposure and poverty in 188 countries. Nature communications, 13(1): 1-11. https://doi.org/10.1038/s41467-022-30727-4

Romanescu G., Hapciuc O. E., Minea I., Iosub M. (2018) Flood vulnerability assessment in the mountain–plateau transition zone: a case study of Marginea village (Romania). Journal of Flood Risk Management, 11: S502–S513. https://doi.org/10. 1111/jfr3.12249

Roșca S., Petrea D., Bilașco Ș., Ioan Rus A., Irimuș I., Fodorean I., Iuliu Vescan L. (2014) Assessment of flood hazard and risk using GIS and historical data. Case-study: the Niraj River Basin (Transylvania Depression, Romania). Conference Proceedings-Photogrametry and Remote Sensing, Cartography and GIS, 3: 497-504

Smit B., Wandel J. (2006) Adaptation, adaptive capacity and vulnerability. Global Environmental Change, 16: 282-292. https://doi.org/10.1016/j.gloenvcha.2006.03.008

Stoica-Fuchs B. (2021) Assessing the vulnerability of transport network to flood hazard using GIS analysis. Case study along Orient-East Med TEN-T Corridor, on Timiș-Cerna Valley, Romania. Present Environment and Sustainable Development, 15(2): 146–160. https://doi.org/10.15551/pesd2021152012

Tanoue M., Hirabayashi Y., Ikeuchi H (2016) Global-scale river flood vulnerability in the last 50 years. Scientific reports, 6(1): 1-9. https://doi.org/10.1038/srep36021

Török I. (2018) Qualitative assessment of social vulnerability to flood hazards in Romania. Sustainability, 10(10). https://doi.org/10.3390/su10103780

Țîncu R., Zêzere J. L., Crăciun I., Lazăr G., Lazăr I. (2020) Quantitative micro-scale flood risk assessment in a section of the Trotuș River, Romania. Land Use Policy, 95: 103881. https://doi.org/10.1016/j.landusepol.2019.02.040

UNDRR (United Nations Office for Disaster Risk Reduction Site) (2022) Terminology. Online glossary, available online at https://www.undrr.org/ terminology

Villagrán de Léon J. C. (2006) Vulnerability: a conceptual and methodological review. Bonn: UNU

Institute for Environment and Human Security, UNU-EHS Source, 4, available online at https://collections.unu.edu/view/unu:1871#viewAttachments

WHO (2020) [https://www.who.int/health-topics/floods?fbclid=IwAR1xDiSs8WlRLVyrZzK68m-3lyEQkmD_RIz7a0vva4sqOaVBFFWvR4vZ0#tab=tab_1], Accessed on 09.12.2022

Willroth P., Diez J. R., Arunotai N. (2011) Modelling the economic vulnerability of households in the Phang-Nga Province (Thailand) to natural disasters. Natural hazards, 58(2): 753-769. DOI: https://doi.org/10.1007/s11069-010-9635-1

Zaharia L., Costache R., Prăvălie R., Minea G. (2015) Assessment and mapping of flood potential in the Slănic catchment in Romania. Journal of Earth System Science, 124(6): 1311-1324.

Zaharia L., Ioana-Toroimac G. (2017) Overview of river-induced hazards in Romania: Impacts and management. In International Symposium on Water in Environment. Springer, Cham. 197-211. https://doi.org/10.1007/978-3-319-79014-5_9

GeoPatterns, Vol. VII (2022), pp. 45-53, https://doi.org/10.5719/GeoP.7/4

Exploring Risk Perception in the Romanian Covid-19 Pandemic

DANIELA DOBRE, IULIANA ARMAS

Faculty of Geography, University of Bucharest
daniela.dobre8@s.unibuc.ro

Abstract. Knowing how a crisis is perceived by a population can lead to more optimal and effective measures to combat negative effects of disasters in this context, attitudes, the degree of involvement, the speed of accepting imposed measures, play an important role for a preventive, pro-active behaviour of both *individual-* and *community-level*. In this paper, based on the data provided by a quantitative questionnaire applied in two non-sequential waves (177 responses in Wave 1 and 368 responses in Wave 5), some aspects of the five constructs expressing the types of perception towards authorities, support, risk of illness, duration of the COVID-19 pandemic, media and some of the factors that may influence perception (personality, cognitive-attitudinal, emotional, behavioural, demographic aspects) are analysed.

Keywords: psychometric research, Covid-19 perception, behaviour, transversal method

1. INTRODUCTION

2021 was the most complicated year in the Romanian medical history and the most relevant event regarding the impact of pandemic in a society, on various socio-economic and psychological aspects (IRES 2021 Opinion Survey). COVID-19 pandemic caused 67,310 deaths, 3,301,662 confirmed cases of illness, 3,224,477 patients were cured, with a mortality of 2.26% (www. worldometers.info, 12.12.2022). On the other hand, a nation-wide opinion survey showed that the psycho-emotional impact of the COVID-19 pandemic led to increased levels of anxiety (10%) and stress (7%), 14% of interviewed subjects declaring they are constantly worried. 50% of the survey participants reported that their everyday life has negatively changed due to restrictions and movement limitations (26%), limitations imposed on their social interaction (12%), job loss (20%), negatively affecting income (8%), health problems (5%), limiting access to medical services (4%), inadequate online education (5%) (IRES, 2021).

2. CONCEPTUAL BACKGROUND

A literature review reveals that psycho-social mechanisms are related to individual perceptions (e.g., Armas and Avram, 2009; Lanciano et al., 2020; Walker and McCane, 2020; Lin et al., 2020; Vancea and Apostol, 2021; Passavanti et al., 2021; Shokrkon and Nicoladis, 2021; Ert et al., 2022; Hagger and Hamilton, 2022). An analysis of psycho-social dimensions of risk perception and behaviour is necessary to determine how perceived risk is related to engagement in protective, pro-active behaviours. Individual perception is built on psychosocial voluntary or involuntary mechanisms, as coping reactions and defence. Perception needs time to develop, is the result of past experiences, is selective, is both subjective and objective, it changes, evolves over time, and is influenced by personal motivations and interests. Perceptions can lead to an action as response or not. In figure 1 there are captured some of the relationships between different types of perceptions and personalities, and the factors that influence perception. Personality can contribute to mental health deterioration, in literature being analysed different coping mechanisms: agreeableness, openness, neuroticism, extraversion, conscientiousness (Lovibond, 1995; Mertens et al, 2020; Walker, 2020; Wissmath, 2021; Hagger, 2022).

Both perception and behavior and/or response evolve over time, the dynamics of this relationships being of interest (Figure 2).

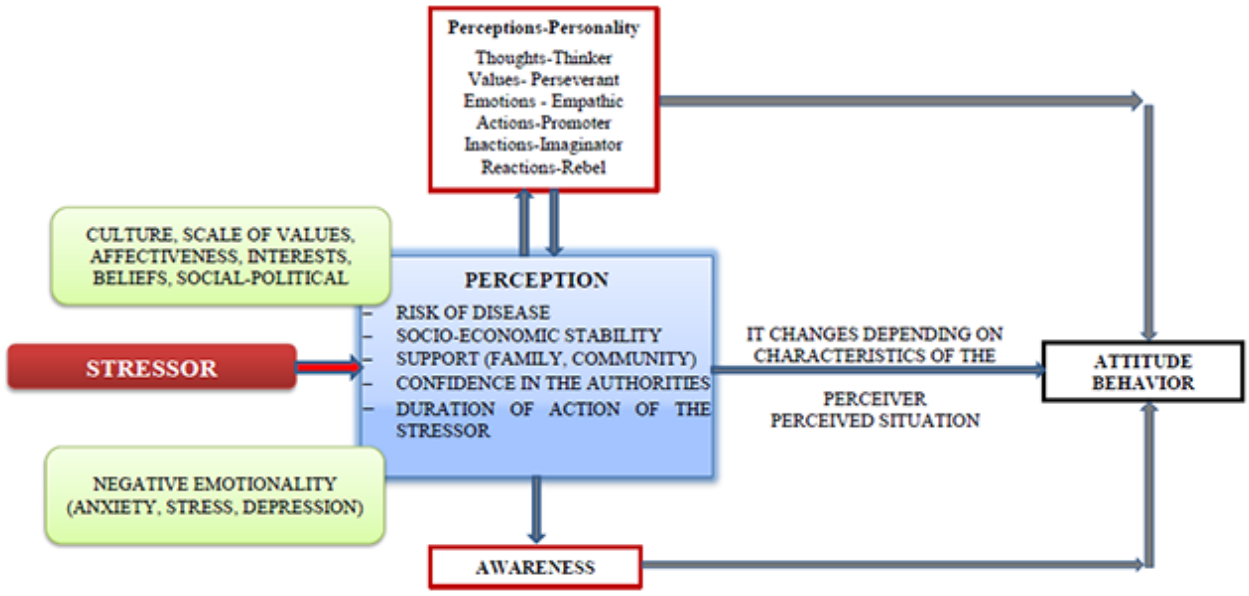

Figure 1. *Conceptual scheme Stressor-Perception-Behavior (personal compilation)*

In the COVID-19 pandemic context, it is a difficult task to understand if people plan to adopt certain coping behaviours or not. It is important that people understand the existence of benefits gained by acting, and for scientists to identify the barriers that block preventive behavior, and the nature of surrounding influences. This study is based on the theory of planned behavior (Ajzen, 1991; Hagger, 2022). According to this theory, if benefits are not lacking and barriers are minor, people will change their behaviours or at least there will be an intention to change. But there is a gap between intention and action, and this should be a possible outcome of the interplay between habits, conditionings and influences.

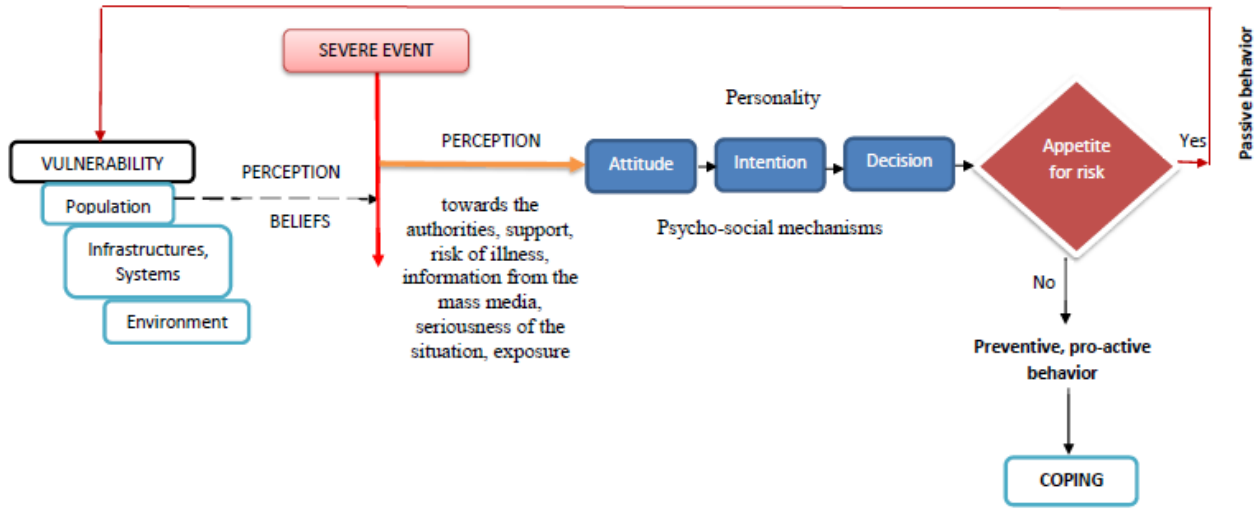

Figure 2. *The role of perception and its post-event evolution*

3. METHODS AND DATA

In this study we used the transversal survey method that allowed us to identify psycho-social mechanisms activated at a certain moment. The on-probability snowballs sampling technique was applied (Heckathorn, 2015).

Date were collected starting with the first wave between March and May 2020 (177 responses). In the 5th wave (2022), we had a sample of 368

subjects. It would have been interesting to have a second opinion from the same subjects after a period, but the lack of data led to a single comparative analysis between two cross-sectional statistical analyses.

The data collection instrument consisted of a 6-part questionnaire, most of the answers being given using a 4- or 5-step Likert-type scale. The structure of the questionnaire is the following: Part I – Perception towards the authorities, support, risk of illness, mass-media, severity of the pandemic threat, exposure, duration of the COVID-19 pandemic, locus of control; Part II – Personality Traits (Neuroticism and Conscientiousness, Iliescu et al. 2015); Part III – DASS Scale (Lovibond, 1995); Part IV – Fear Scale (Mertens et al, 2020); Part V – Behavior (Ajzen, 1991) and Part VI – relevant socio-demographic data.

Sample statistics are given in Table 1 and Table 2 and Figure 3.

Table 1. Pandemic wave 1, demographic data (percentages)

Sex	Age		Higher education	Occupation	Location in urban areas	Property type	Block of flats	Income > average	Religious
women	20-29	>50		employees		homeowners			
64	44	15	66	61	74	84	60	44	72

Table 2. Pandemic wave 5, demographic data (percentages)

Sex	Age		Higher education	Occupation	Location in urban areas	Property type	Block of flats	Income > average	Religious
women	20-29	>50		employees		homeowners			
62	34	21	66	64	76	88	58	43	74

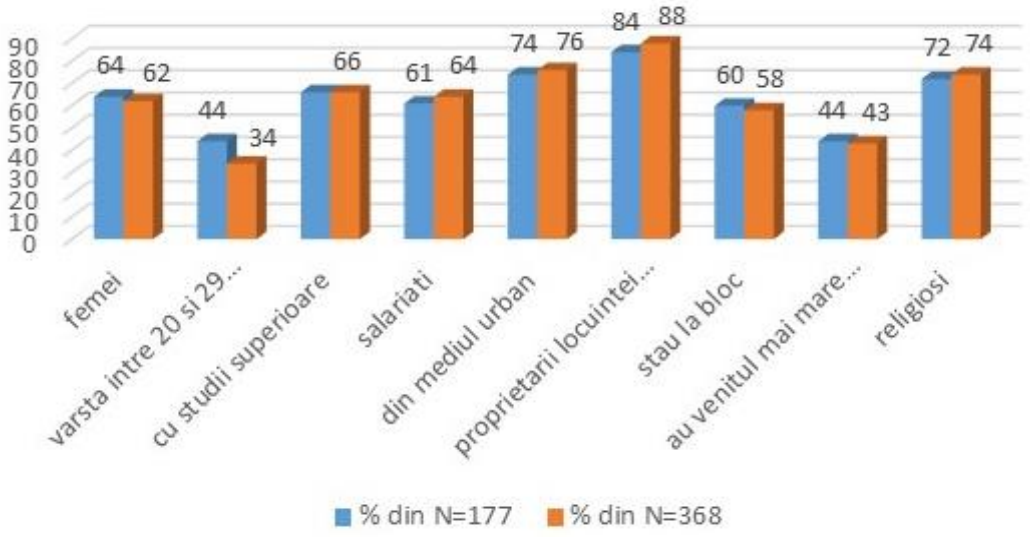

Figure 3. *Comparison of socio-demographic characteristics (%)*

Different methods (correlations, covariance, path and modelling of structural equations) were performed in order to examine the relationships between the level of perception, socio-demographic characteristics, sources of information, education, experience, emotional states (fear, anxiety, stress), personality, gender and behavior. After designing the conceptual schemes, these schemes were tested, verifying the fulfilment of the criteria for matching the model to the data (Kenny, 2014, 2020; Suhr, 2022; Byrne, 2012).

4a. RESULTS. DESCRIPTIVE STATISTICS

Selected comparative results on perception and thrust, compliance with directives, and different behaviours are shown in tables 3 to 6.

Table 3a – Perception (wave 1): To what extent do you trust the information regarding COVID-19 provided by…

	Mean (SD)	(%)				
		1- to a very small extent	2- small/reduced extent	3- moderate extent	4- large extent	5- to a very large extent
TV	2.33 (1.19)	31.07	27.12	25.99	9.60	6.21
Newspapers (paper or online)	2.33 (1.15)	28.81	31.07	23.16	12.43	4.52
The strategic information group	3.03 (1.31)	14.12	24.29	22.60	22.03	16.95
Internet news	2.14 (1.10)	36.16	29.38	22.60	8.47	3.39
Facebook and other social networking sites	1.79 (1.08)	55.37	22.60	12.99	5.65	3.39
People around you	2.76 (1.21)	19.21	23.16	27.12	23.16	7.34

Table 4a – Perception (wave 1): How much do you trust the following institutions that they are managing the COVID-19 crisis well?

	Mean (SD)	(%)				
		1- to a very small extent	2- small/reduced extent	3- moderate extent	4- large extent	5- to a very large extent
The president	2.35 (1.18)	32.77	20.34	31.07	10.73	5.08
Government	2.01 (1.07)	42.94	23.73	26.55	3.39	3.39
Health system	2.92 (1.23)	14.69	23.73	28.81	20.34	12.43
Ministry of Interior	2.44 (1.25)	28.81	25.99	26.55	9.60	9.04
Army	2.88 (1.36)	22.60	16.95	25.99	19.21	15.25
DSU/ISU	2.98 (1.38)	19.77	20.34	18.64	24.29	16.95
Police	2.57 (1.29)	28.81	18.08	29.38	14.69	9.04

Table 5a – Behavior (wave 1): To what extent do you consider that you comply with the directives of the authorities to stay at home during the state of emergency?

	Mean (SD)	(%)				
		1- to a very small extent	2- small/reduced extent	3- moderate extent	4-large extent	5- to a very large extent
Individual	4.19 (0.87)	1.69	1.69	14.69	40.11	41.81

Table 6a – Behavior (wave 1): How often do you leave the household?

	Mean (SD)	(%)					
		daily	Once every 2-3 days	Once a week	Once every 2 weeks	Once every 3 weeks	Less often
individual behavior	1.58(1.02)	64.61	23.16	7.34	2.26	0.56	2.26

The same variables in Wave 5 are presented below (table 3b to table 6b) and a comparison between the acceptance of pandemic measures imposed by the authorities is drown in figure 4.

Table 3b – Perception (wave 5): To what extent do you trust the information regarding COVID-19 provided by…

	Mean (SD)	(%)				
		1- to a very small extent	2- small/reduced extent	3- moderate extent	4- large extent	5- to a very large extent
TV	2.38 (1.15)	28.5	25.3	30.4	10.9	4.9
Newspapers (paper or online)	2.38 (1.12)	25.8	31	26.6	12.2	4.3
The strategic information group	3.04 (1.30)	14.7	20.9	26.9	20.4	17.1
Internet news	2.21 (1.09)	32.3	30.4	24.7	9.2	3.3
Facebook and other social networking sites	1.88 (1.05)	48.4	25.8	17.7	5.4	2.7
People around you	2.77 (1.20)	18.5	22.8	30.2	20.7	7.9

Table 4b – Perception (wave 5): How much do you trust the following institutions that they are managing the COVID-19 crisis well?

	Mean (SD)	(%)				
		1- to a very small extent	2- small/reduced extent	3- moderate extent	4- large extent	5- to a very large extent
The president	2.12 (1.17)	42.9	19.6	23.9	10.1	3.5
Government	1.91 (1.03)	47.8	22	23.1	5.4	1.6
Health system	3.09 (1.22)	11.1	21.7	28.8	23.6	14.7
Ministry of Interior	2.34 (1.24)	33.2	24.2	25.3	10.1	7.3
Army	2.69 (1.34)	27.2	18.2	24.2	19.6	10.9
DSU/ISU	2.97 (1.38)	20.9	16.8	22.8	23.1	16.3
Police	2.40 (1.26)	33.4	19.3	27.7	12.8	6.8

Table 5b – Behavior (wave 5): To what extent do you consider that you comply with the directives of the authorities to stay at home during the state of emergency?

	Mean (SD)	(%)				
		1- to a very small extent	2- small/reduced extent	3- moderate extent	4- large extent	5- to a very large extent
Individual	4.21 (0.87)	0.8	2.4	16.8	34.2	45.7

Table 6b- Wave 5: How often do you leave the household?

	Mean (SD)	(%)					
		daily	Once every 2-3 days	Once a week	Once every 2 weeks	Once every 3 weeks	Less often
individual behavior	1.5(1.0)	64.1	24.5	7.1	1.6	0.3	2.4

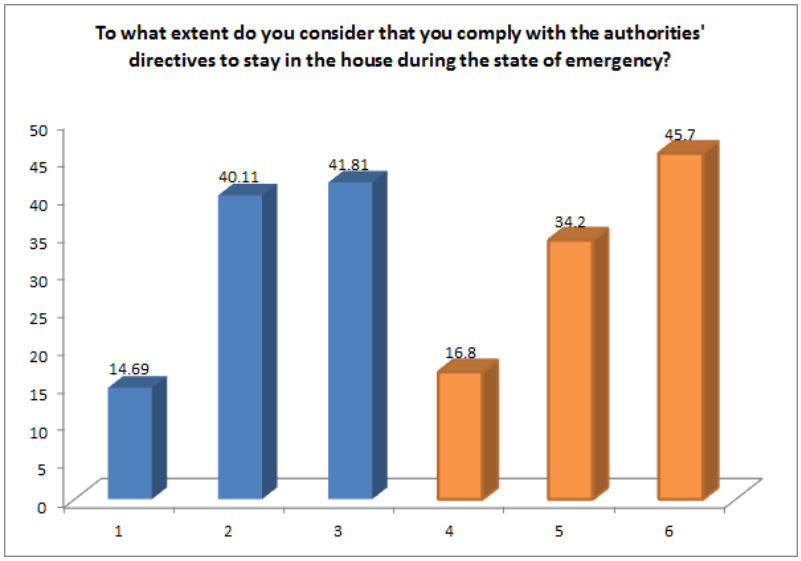

Figure 4. *Comparison between acceptance of pandemic authority measures (wave 1 in blue vs. wave 5 in orange)*

4b. RESULTS. INFERENTIAL STATISTICS

Our working hypothesis was that the level of perception plays a role in the attitude and behaviour of selected subjects during the COVID-19 lockdown restrictions. Path and structural analysis tested relationships between measured and latent variables, using a measured and a structural model (Kenny, 2014, 2020; Suhr, 2022; Grace, 2022; Beran and Violato, 2010).

Methodological steps are: (1) definition of independent and dependent variables, (2) model identification, (3) parameter estimation, (4) model-fitting, (5) model redefinition and (6) interpretation of results. The fit of the model to the measured data is obtained using some parameters such as the chi-square test, the comparative fit index (CFI), the mean square error of approximation (RMSEA) related to the residual in the model.

Some exemplification of modelling "reasonably consistent to the data" are described below and, although not all modelling is presented, some of the results will be emphasised in figures 5 to 10:

- mass media is a better predictor for how directives from the public authority are respected and adopted, reducing fear and increasing coping activities. On the other hand, the situation presented by the authorities negatively influences the confidence in receiving adequate care and overcoming illness, leading to coping through other mechanisms, Figure 5;
- the situation presented by officials negatively influences how directives from the public authority are respected and the confidence in receiving adequate care is affected. Coping is based on the believe that in the event of an illness one will get support from friends and family. Coping does not significantly relate from compliance with imposed measures, and negative emotions do not influence it;
- fear of COVID-19 is a good predictor of the psychological states, neuroticism and stress (with direct and indirect effects); fear does not strongly influence the perception of exposure to illness, which in turn correlates negatively with stress. Thus, stress is saturated by another variable, not by the perceived exposure;
- Information given by public authorities does not influence neuroticism and anxiety; psychological states influence each other significantly, depression being a good predictor for anxiety and anxiety a predictor for stress; psychological effects do not correlate with perceptions of information given by officials, Figure 6;
- psychological effects are a very good predictor, in a directly proportional relationship, for the perception of illness, and the received messages from the authorities. What is worth mentioning in this model is that the perception of exposure

to the risk of disease is not a significant predictor of fear and the neuroticism personality type, but of the perception of the exaggerations made by authorities and the lack of support. The lack of support is associated with the lack of medical care, leading to the conclusion that there is no trust in the administrative and health system, Figure 7.

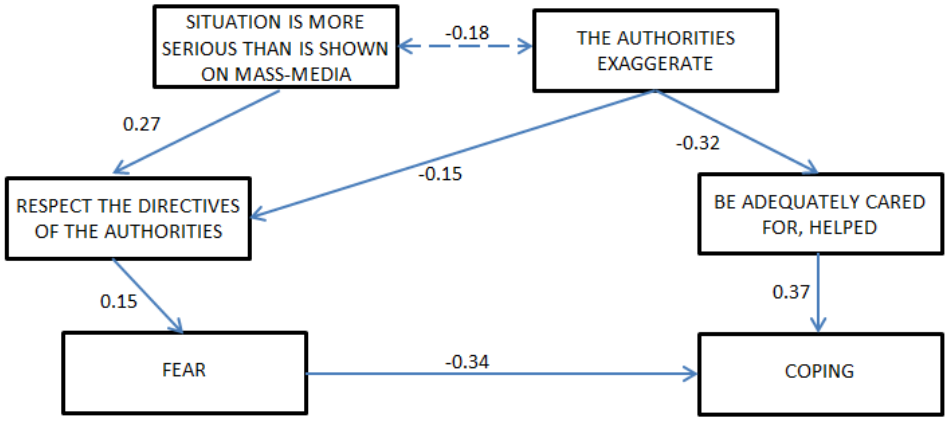

RMSEA = 0.028, SRMR = 0.042; CFI = 0.988, TLI = 0.978, GFI = 0.999

***Figure 5**. The extent of relationships considered between the observed variables: mass-media, directives and measures from the public authority, trust, coping*

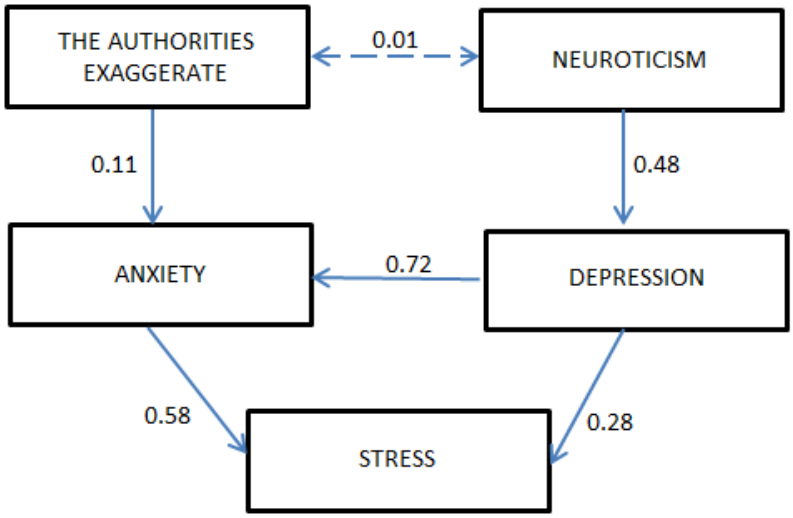

RMSEA = 0.218, SRMR = 0.071; CFI = 0.913, TLI = 0.805, GFI = 0.948

***Figure 6**. The extent of the relationships considered between the observed variables: perception and psychological states (fear, stress, anxiety)*

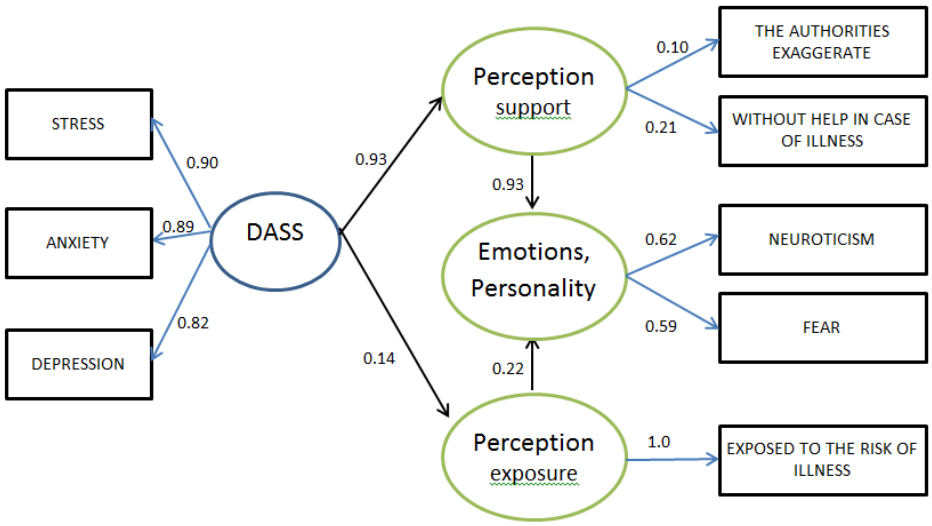

RMSEA = 0.120; SRMR = 0.062; CFI = 0.914, TLI = 0.859

***Figure 7**. The relationships between the observed and latent variables: psychological effects, perception, directives from the public authority, emotions, personality, support*

5. CONCLUSIONS

It is widely accepted that understanding risk perceptions can lead to more effective coping measures to mitigate negative effects of disasters. Our study results highlighted, for instance, that mass-media has a more important role in informing the population than the authorities. With this awareness, involving mass media in tailored communication strategies plays a central role for governments seeking to efficiently inform, and communicate in crises and disasters for triggering behavioural changes. On the other hand, the perception of pandemic COVID-19 risks correlates with emotional and personality features and less with cognitive and demographic characteristics such as education, gender, age. The applied inferential statistical analysis cannot establish causalities (these only resulting from longitudinal studies, or experiments). We emphasise that the aim of the presented analyses was not to find models with full statistical significance, but only to fit the models to be reasonably consistent with the data.

Regarding the modeling of the structural equations, inversely proportional relationships are observed between psychological effects (fear, stress, anxiety) and the degree of education, information, and coping. Interesting is the fact that, on the other hand, coping does not have as consistent predictors education and directives and measures from the public authority, etc. A significant negative correlation is recorded between the perception of the expected support in case of illness and the extent to which professional care will be received. At the same time, negative emotions are a better predictor for coping than the support given by the health system.

In case of disasters we have developed mitigation plans, but we still lack psychological coping strategies for the affected human dimensions. After a pandemic, we don't have only to rebuild and improve infrastructures, we also have to build and maintain our well-being.

REFERENCES

Ajzen, I. (1991) The Theory of Planned Behavior. Organizational Behavior and Human Decision Processes, 50, 179-211. https://people.umass.edu/aizen/tpbrefs.html.

Albarracin D., Johnson B. T., Fishbein M., Muellerleile P. A. (2001) Theories of Reasoned Action and

Planned Behavior as Models of Condom Use: A Meta-Analysis, Psychological Bulletin 2001, Vol. 127, No. 1, 142-161, doi: 10.1037//0033-2909. 127.1.142.

Armas I., Avram E. (2009) Perception of flood risk in Danube Delta, Romania, Nat. Hazards, 50:269–287, doi 10.1007/s11069-008-9337-0.

Byrne M. B. (2012) Structural Equation Modeling with Mplus.Basic Concepts, Applications, and Programming, Routledge, Taylor & Francis Group.

Ert E., Melkonyan T., Trautmann S.T. (2022) Contagious Risks: Perception, Behavior, and Management – Lessons from the COVID-19 Pandemic. Front. Psychol. 12:835088, doi: 10.3389/fpsyg.2021.835088

Hagger M. S., Hamilton K. (2022) Social cognition theories and behavior change in COVID-19: A conceptual review, Behaviour Research and Therapy, Volume 154, 104095, ISSN 0005-7967, https://doi.org/10.1016/j.brat.2022.104095.

Heckathorn D.D. (2015) Snowball Versus Respondent-Driven Sampling. Sociol Methodol 41(1): 352-366.

Iliescu, D., Popa, M., & Dimache, R. (2015). Adaptarea românească a Setului International de Itemi de Personalitate: IPIP-Ro [The Romanian adaptation of the International Personality Item Pool: IPIP-Ro]. Psihologia Resurselor Umane, 13(1), 83-112.

James Benjamin Grace, General guidance for custom-built structural equation models, One Ecosystem 7, 2022, https://doi.org/10.3897/oneeco.7.e72780.

Kenny D. A. (2020) Measuring Model Fit, http://www.davidakenny.net/cm/fit.htm.

Lanciano T., Graziano G., Curci A., Costadura S., Monaco A. (2020) Risk perceptions and psychological effects during the Italian COVID-19 Emergency. Front. Psychol. 11:580053. doi: 10.3389/fpsyg.2020.580053

Lin C.Y., Imani V., Majd N.R., Ghasemi Z., Griffiths M.D., Hamilton K., Hagger M.S., Pakpour A.H. (2020) Using an integrated social cognition model to predict COVID-19 preventive behaviours. Br J Health Psychol. 25(4):981-1005, doi: 10.1111/bjhp.12465. PMID: 32780891; PMCID: PMC7436576.

Lovibond, S.H. &Lovibond, P.F. (1995) Manual for the Depression Anxiety & Stress Scales.(2nd Ed.) Sydney: Psychology Foundation.

Passavanti M., Argentieri A., Barbieri D.M., Lou B., Wijayaratna K., ForoutanMirhosseini A.S., Wang F., Naseri S., Qamhia I., Tangerås M., Pelliciari M., Ho C.H. (2021) The psychological impact of COVID-19 and restrictive measures in the world. J. Affect Disord. 2021 Mar 15; 283:36-51. doi: 10.1016/j.jad.2021.01.020. Epub 2021 Jan 15.

Shokrkon A, Nicoladis E. (2021) How personality traits of neuroticism and extroversion predict the effects of the COVID-19 on the mental health of Canadians, PLoS ONE 16(5), https://doi.org/10.1371/journal.pone.0251097

Suhr D. (2022) The Basics of Structural Equation Modeling, University of Northern Colorado, https://www.lexjansen.com/wuss/2006/tutorials/TUT-Suhr.pdf.

Vancea F., Apostol M. Ș. (2021) Changes in mental health during the COVID-19 crisis in Romania: A repeated cross-section study based on the measurement of subjective perceptions and experiences, SciProg. 104(2):368504211025873. doi: 10.1177/00368504211025873.

Walker G., McCabe T. (2020) Psychological defence mechanisms during the COVID-19 pandemic: A case series. Eur J Psychiatry. 35(1):41-45. 2021, doi: 10.1016/j.ejpsy.2020.10.005.

Wissmath B., Mast F.W., Kraus F, Weibel D. (2021) Understanding the psychological impact of the COVID-19 pandemic and containment measures: An empirical model of stress. PLoS ONE 16(7): e0254883. 2021, https://doi.org/10.1371/journal.pone.0254883

https://www.worldometers.info/coronavirus/country/romania

Volume 7, 2022

CRMD

GeoPatterns

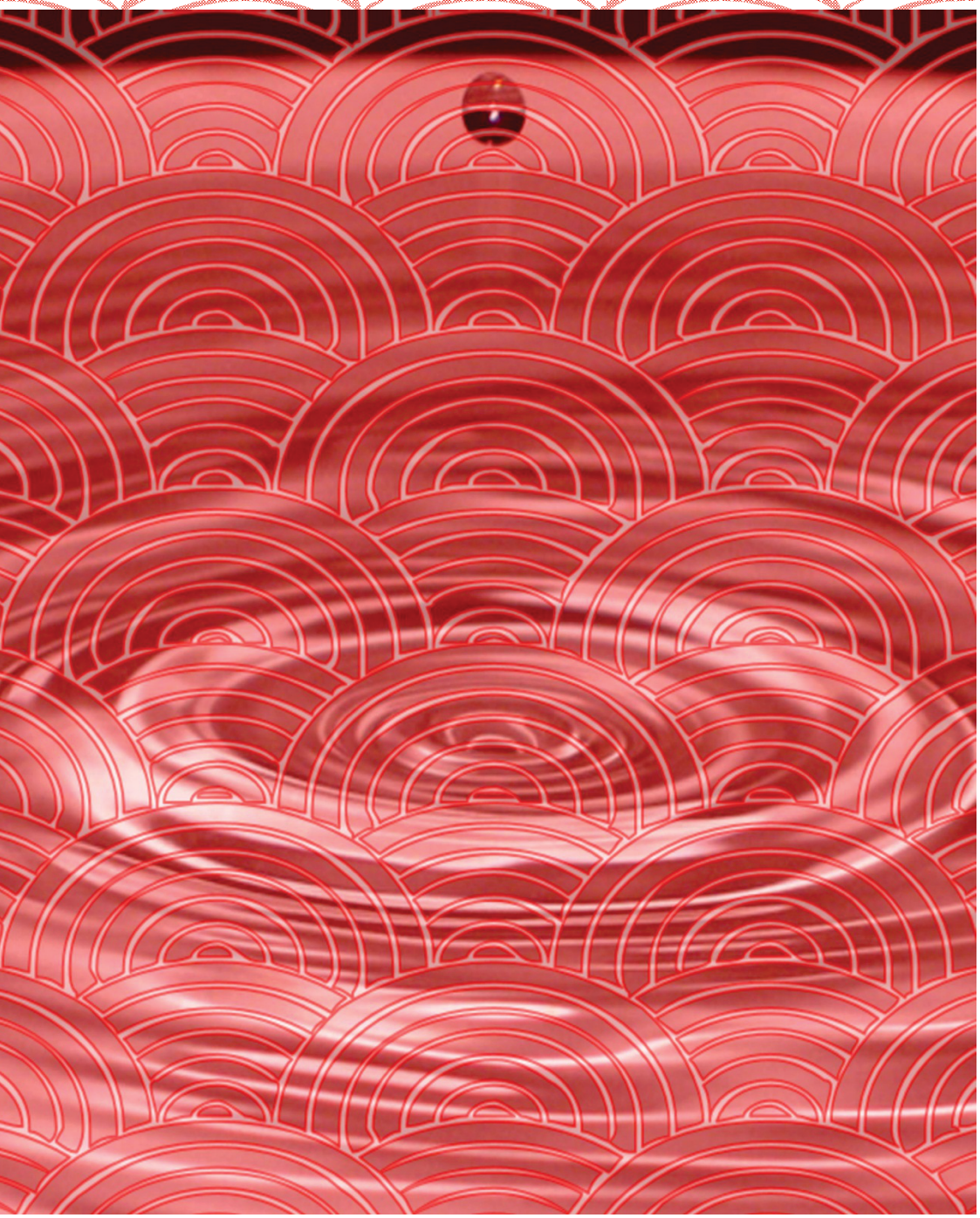

"Science is the millennial endeavor to identify the underlying patterns that form our world and explains the interconnectedness of the natural and social systems."

9 772501 783706

EDITURA UNIVERSITĂȚII DIN BUCUREȘTI
BUCHAREST UNIVERSITY PRESS